

# Fermionic Casimir densities for a uniformly accelerating mirror in the Fulling-Rindler vacuum

A. A. Saharian<sup>1\*</sup>, L. Sh. Grigoryan<sup>2</sup>, V. Kh. Kotanjyan<sup>1,2</sup>

<sup>1</sup>*Institute of Physics, Yerevan State University,  
1 Alex Manoogian Street, 0025 Yerevan, Armenia*

<sup>2</sup>*Institute of Applied Problems of Physics NAS RA,  
25 Hrachya Nersisyan Street, 0014 Yerevan, Armenia*

April 22, 2026

## Abstract

We investigate the local characteristics of the Fulling-Rindler vacuum for a massive Dirac field induced by a planar boundary moving with constant proper acceleration in  $(D + 1)$ -dimensional flat spacetime. On the boundary, the field operator obeys the bag boundary condition. The boundary divides the right Rindler wedge into two separate regions, called RL and RR regions. In both these regions, the fermion condensate and the vacuum expectation value (VEV) of the energy-momentum tensor are decomposed into two contributions. The first one presents the VEVs in the Fulling-Rindler vacuum when the boundary is absent and the second one is the boundary-induced contribution. For points away from the boundary, the renormalization is reduced to the one for the boundary-free geometry. The total VEVs are dominated by the boundary-free parts near the Rindler horizon and by the boundary-induced parts in the region near the boundary. For a massive field the boundary-free contributions in the fermion condensate and the vacuum energy density and effective pressures are negative everywhere. The boundary-induced contributions in the fermion condensate and the energy density are positive in the RL region and negative in the RR region. For a massless field the fermion condensate vanishes in spatial dimensions  $D \geq 2$ , while the VEV of the energy-momentum tensor is different from zero. This behavior contrasts with that of the VEVs in the Minkowski vacuum for the geometry of a boundary at rest relative to an inertial observer. In the latter case, the fermion condensate for a massless field is nonzero, while the VEV of the energy-momentum tensor becomes zero. The obtained results are used to investigate the VEV of the fermionic energy-momentum tensor in weak gravitational fields and background geometries that are conformally related to Rindler spacetime.

Keywords: Fulling-Rindler vacuum, Casimir effect, Dirac field, uniformly accelerating mirror

## 1 Introduction

The Rindler coordinates  $x^\mu = (\tau, \rho, x^2, \dots, x^D)$  in  $(D + 1)$ -dimensional flat spacetime, with the variation range  $\tau \in (-\infty, +\infty)$ ,  $\rho \in [0, \infty)$ ,  $x^i \in (-\infty, +\infty)$ ,  $i = 2, \dots, D$ , realize the reference frame of uniformly accelerated observers. They are related to the Minkowskian coordinates  $x'^\mu = (x'^0 = t, x'^1, x'^2, \dots, x'^D)$  of inertial observers by the coordinate transformation

$$t = \rho \sinh \tau, \quad x^1 = \rho \cosh \tau, \quad x^i = x^i, \quad i = 2, \dots, D. \quad (1.1)$$

---

\*E-mail: saharian@ysu.am

With this transformation, the line element in the Rindler coordinates reads

$$ds_{\text{R}}^2 = g_{\mu\nu} dx^\mu dx^\nu = \rho^2 d\tau^2 - d\rho^2 - d\mathbf{x}^2, \quad (1.2)$$

where  $\mathbf{x} = (x^2, x^3, \dots, x^D)$ . The worldlines  $\rho = \text{const}$  and  $\mathbf{x} = \text{const}$  describe a uniformly accelerating observer following the trajectory parallel to the  $x^1$  axis and having a proper acceleration  $1/\rho$ . The proper time  $\tau_{\text{p}}$  of the observer is expressed in terms of the dimensionless time coordinate  $\tau$  as  $\tau_{\text{p}} = \rho\tau$ . The hyperplanes  $x^1 = \pm t$  are horizons for Rindler observers. They divide the Minkowski spacetime into four wedges. For the coordinates defined in (1.1) one has  $x^1 > |t|$  and they correspond to the so called Right (R) region. The coordinate transformation in the wedge  $x^1 < -|t|$  (Left (L) region) is given by (1.1) with  $x^1 = -\rho \cosh \tau$ . The remaining wedges  $t > |x^1|$  and  $t < -|x^1|$  present the Future (F) and Past (P) regions of the Minkowski spacetime. The corresponding transformations read  $t = \pm \rho \cosh \tau$ ,  $x^1 = \rho \sinh \tau$ .

The interest to the Rindler spacetime, as a background geometry in quantum field theory, is motivated by a number of reasons. First of all, the Rindler geometry is a classic example for discussing fundamental issues such as the observer dependence of the concepts of vacuum and particles. The Rindler metric tensor is static and the canonical quantization of a given field can be realized by using the modes of a given energy in both Rindler and Minkowskian coordinates. Expanding the field operator over those modes, the vacuum and particle states are constructed following the standard procedure. It turns out that the vacuum states constructed on the basis of Rindlerian and Minkowskian modes (Fulling-Rindler and Minkowski vacua, respectively) are different (see, for example, [1, 2, 3]). An observer moving with constant acceleration registers Rindler quanta in the Minkowski vacuum (the Unruh effect [4, 5, 6]), and an inertial observer registers particles in the Fulling-Rindler vacuum. The simplest example of the system registering particles is the Unruh-de Witt point like detector [1]. An important difference between Rindler observers and inertial observers is the presence of an event horizon related to the accelerated motion. The presence of the horizon introduces new qualitative features in quantum field-theoretical effects. The relative simplicity of the Rindler geometry allows to obtain closed analytical results for physical characteristics describing the state of a quantum field. This helps to understand the consequences of the existence of a horizon in more complex situations in curved space-time, including those for de Sitter and black hole geometries. An interesting quantum phenomena is the entanglement between the states in the regions separated by horizons. In the Rindler geometry the worldlines of uniformly accelerating observers are located in the right and left wedges. For those observers, the Minkowski vacuum is an entangled state that connects the states in separate wedges (see, for example, [7]-[10] and references therein).

An intriguing macroscopic manifestation of the non-trivial physical properties of the quantum vacuum is the Casimir effect (for reviews see [11]-[14]). It is a boundary-induced phenomenon caused by the influence of boundaries on quantum fluctuations of fields. The effect has been thoroughly investigated for both bosonic and fermionic fields and for various geometries of boundaries and background spacetime. A series of high-precision experiments confirm the Casimir effect for electromagnetic field in problems involving conducting and dielectric boundaries. An interesting topic in the investigations on the Casimir effect is the dependence of the expectation values of physical quantities on the chosen vacuum state. In the present paper we study the Casimir contributions in the fermion condensate and the mean energy-momentum tensor for Dirac field, induced by a planar boundary moving with constant proper acceleration through the Fulling-Rindler vacuum state (quantum fermionic fields in Rindler spacetime have been considered in various aspects in the literature, see, e.g., Refs. [15]-[32]). Similar studies have been conducted previously in Refs. [33]-[38] for scalar and electromagnetic fields in the geometry of a single and two parallel planar boundaries. Note that the problems of the Fulling-Rindler vacuum polarization by moving boundaries are closely related to the investigation of the Casimir effect in weak gravitational fields (see, for example, Refs. [39]-[50]).

The organization of the paper is as follows. The problem setup and the Dirac modes in the RR and RL regions, separated by a mirror, are presented in the next section. In Section 3 we investigate the fermion condensate in those regions. The boundary-induced contributions are explicitly separated

and their behavior in asymptotic regions of the parameters is studied. The corresponding investigation for the expectation value of the energy-momentum tensor is given in Section 4. The main results are summarized in Section 6. In Appendix A we present the details of the evaluation of the normalization integrals in the RR and RL regions. In Appendix B, by using the generalized Abel-Plana formula, a summation formula is derived for the series appearing in the expressions of the expectation values in the RR-region. The proof of the identities, used for the separation of the boundary-induced contributions in the expectation values for the RL-region, is presented in Appendix C.

## 2 Problem setup and fermionic modes

### 2.1 Problem setup

Consider a fermionic field  $\psi(x^\mu)$  in background of spacetime described by the line element (1.2). The  $(D + 1)$ -bein fields will be taken in the form  $e_{(0)}^\mu = \delta_0^\mu/\rho$ ,  $e_{(b)}^\mu = \delta_b^\mu$ ,  $b = 1, 2, \dots$ , and for the covariant components of the metric tensor,  $g_{\mu\nu} = \eta_{ab}e_\mu^{(a)}e_\nu^{(b)}$ , one has  $g_{\mu\nu} = \text{diag}(\rho^2, -1, \dots, -1)$ . Here,  $\eta_{ab}$  is the Minkowskian metric tensor in Cartesian coordinates with  $a, b = 0, 1, \dots, D$ . The field operator obeys the Dirac equation

$$(i\gamma^\mu\nabla_\mu - m)\psi = 0, \quad \nabla_\mu = \partial_\mu + \Gamma_\mu, \quad (2.1)$$

with the spin connection  $\Gamma_\mu$ . For the  $N \times N$  Dirac matrices in the coordinates  $x^\mu$  we have the relation  $\gamma^\mu = e_{(b)}^\mu\gamma^{(b)}$ , where  $\gamma^{(b)}$  are the flat spacetime gamma matrices in Cartesian coordinates (for the construction of the matrices  $\gamma^{(b)}$  in general number of the spacetime dimension see, e.g., [51, 52]). They obey the anticommutation relation  $\{\gamma^\mu, \gamma^\nu\} = 2g^{\mu\nu}$  and we will assume that the field  $\psi(x^\mu)$  realizes the irreducible representation of this Clifford algebra. For odd values of spatial dimension  $D$ , the irreducible representation is unique (up to a similarity transformation). For even  $D$  one has two inequivalent irreducible representations. The dimension of the Dirac matrices in the irreducible representation is given by  $N = 2^{\lfloor(D+1)/2\rfloor}$ , where  $\lfloor \dots \rfloor$  stands for the integer part of the enclosed expression. Denoting the covariant derivative for vector fields by  $\nabla$ ; the spin connection is expressed as  $\Gamma_\mu = \gamma^{(a)}\gamma^{(b)}e_{(a)}^\nu e_{(b)\nu;\mu}/4$ .

Our main interest is the shift in the vacuum expectation values (VEVs) of the physical characteristics of the Fulling-Rindler vacuum induced by a uniformly accelerated mirror moving along the axis  $x^1$  with a proper acceleration  $1/\rho_0$ . On the boundary  $\rho = \rho_0$  with the normal  $n_\mu$  the Dirac field obeys the bag boundary condition

$$(1 + in_\mu\gamma^\mu)\psi = 0. \quad (2.2)$$

In the MIT bag model of hadrons, this boundary condition is used to confine quarks within a finite volume. It ensures that there is no flux of fermions at the boundary on which the boundary condition is imposed. From this condition, it follows that  $n_\mu j^\mu = 0$  for  $\rho = \rho_0$ , where  $j^\mu = \bar{\psi}\gamma^\mu\psi$  being the current density. Here and below,  $\bar{\psi} = \psi^\dagger\gamma^{(0)}$  is the Dirac conjugate for the field  $\psi$ . Due to the condition (2.2), the boundary  $\rho = \rho_0$  reflects all the fermion modes. In this sense, the boundary can be called a mirror for the Dirac field. In the following, the terms boundary and mirror will be used interchangeably. We assume that the mirror is located in the R wedge of the Rindler geometry. It divides the R region into two subregions: region  $0 \leq \rho < \rho_0$  (RL region) and region  $\rho_0 < \rho < \infty$  (RR region). For the components of the normal in those regions we have  $n_\mu = \delta^{(J)}\delta_\mu^1$  with  $\delta^{(J)} = -1$  in the RR region and  $\delta^{(J)} = 1$  in the RL region. In Fig.1 we plotted the coordinate lines in the R wedge of the Rindler spacetime. The worldline of the mirror, separating the RL and RR regions, is plotted by a thick curve.

As physical characteristics of the fermionic Fulling-Rindler vacuum, the fermion condensate and the expectation value of the energy-momentum tensor will be considered. The evaluation procedure we will employ is based on the summation of the corresponding mode sums over the complete set of fermionic modes. In what follows we specify the mode functions and the eigenvalues of quantum numbers for the RL and RR regions.

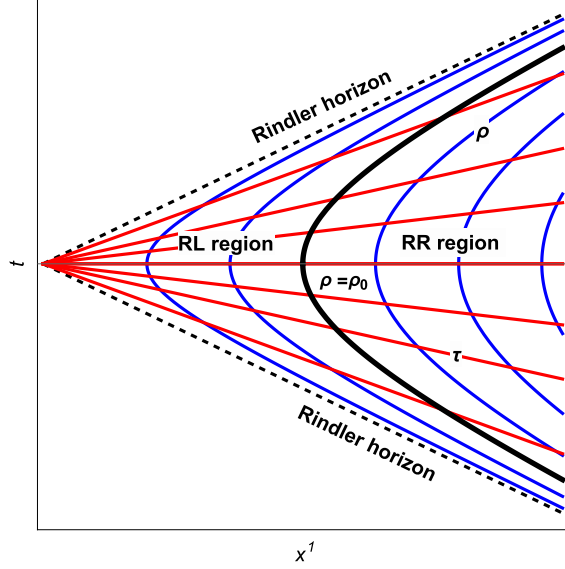


Figure 1: The coordinate lines  $\tau = \text{const}$  and  $\rho = \text{const}$  in the R region of the Rindler spacetime on the plane  $(x^1, t)$ . The worldline of a uniformly accelerating mirror is depicted by a thick line. It separates the RL and RR regions.

## 2.2 Mode functions: General structure

We want to find a complete set of solutions to equation (2.1) for the geometry (1.2) obeying the boundary condition (2.2). The expression for the spin connection is simplified to  $\Gamma_\mu = \delta_\mu^0 \gamma^{(0)} \gamma^{(1)} / 2$ . Following the procedure described in [32], the positive and negative energy modes,  $\psi_\sigma^{(+)}$  and  $\psi_\sigma^{(-)}$ , respectively, are presented in the form

$$\psi_\sigma^{(\pm)}(x^\mu) = N_\sigma e^{\mp i\omega\tau + i\mathbf{k}\cdot\mathbf{x}} Z_{i\omega \mp \frac{1}{2}\gamma^{(0)}\gamma^{(1)}}(\lambda\rho) \chi_\eta^{(\pm)}(\mathbf{k}), \quad (2.3)$$

where  $\mathbf{k} = (k^2, \dots, k^D)$  and the function  $Z_\nu(x)$  is the linear combination of the modified Bessel functions  $I_\nu(x)$  and  $K_\nu(x)$ :

$$Z_\nu(x) = C_{1\sigma} I_\nu(x) + C_{2\sigma} K_\nu(x). \quad (2.4)$$

In (2.3),  $\sigma = (\omega, \mathbf{k}, \eta)$  presents the set of quantum numbers specifying the modes, and

$$\lambda = \sqrt{k^2 + m^2}, \quad k = |\mathbf{k}|. \quad (2.5)$$

The quantum number  $\eta$  specifies the spinorial degrees of freedom. For the energy of the mode (2.3), measured by an observer with fixed spatial coordinates  $(\rho, \mathbf{x})$ , one has  $\varepsilon_\rho = \omega/\rho$ .

The spinors  $\chi_\eta^{(\pm)}(\mathbf{k})$  obey the relation

$$P(\mathbf{k})\chi_\eta^{(\pm)}(\mathbf{k}) = \chi_\eta^{(\pm)}(\mathbf{k}), \quad (2.6)$$

where

$$P(\mathbf{k}) = \frac{1}{2} \left( 1 - i\gamma^{(1)} \frac{\boldsymbol{\gamma}\mathbf{k} + m}{\lambda} \right), \quad \boldsymbol{\gamma}\mathbf{k} = \sum_{i=2}^D \gamma^{(i)} k^i. \quad (2.7)$$

For the operator (2.7), the properties  $P^2(\mathbf{k}) = P(\mathbf{k})$  and  $P^\dagger(\mathbf{k}) = P(\mathbf{k})$  are easily checked. The orthonor-

mality and completeness relations

$$\begin{aligned}\chi_{\eta}^{(\pm)\dagger}(\mathbf{k})\chi_{\eta'}^{(\pm)}(\mathbf{k}) &= \delta_{\eta\eta'}, \\ \sum_{\eta} \chi_{\eta\alpha}^{(\pm)}(\mathbf{k})\chi_{\eta\beta}^{(\pm)\dagger}(\mathbf{k}) &= P_{\alpha\beta}(\mathbf{k}),\end{aligned}\tag{2.8}$$

take place for  $\chi_{\eta}^{(\pm)}(\mathbf{k})$ , with  $\alpha$  and  $\beta$  being spinor indices. In addition, by using (2.6), the property

$$\left(1 + i\gamma^{(1)}\frac{\boldsymbol{\gamma}\mathbf{k} + m}{\lambda}\right)\chi_{\eta}^{(\pm)}(\mathbf{k}) = 0,\tag{2.9}$$

is easily proven.

The boundary condition for the modes (2.3) is written as

$$\left(1 + i\delta^{(J)}\gamma^{(1)}\right)Z_{i\omega\mp\frac{1}{2}\gamma^{(0)}\gamma^{(1)}}(\lambda\rho)\chi_{\eta}^{(\pm)}(\mathbf{k}) = 0.\tag{2.10}$$

By using the relation (see also [15])

$$f(\gamma^{(0)}\gamma^{(1)}) = \frac{1}{2}\sum_{\varkappa=\pm 1}\left(1 + \varkappa\gamma^{(0)}\gamma^{(1)}\right)f(\varkappa),\tag{2.11}$$

for a given function  $f(x)$ , the condition is rewritten as

$$\sum_{\varkappa=\pm 1}\left[1 + \varkappa\gamma^{(0)}\gamma^{(1)} + i\delta^{(J)}\left(\gamma^{(1)} + \varkappa\gamma^{(0)}\right)\right]\chi_{\eta}^{(\pm)}(\mathbf{k})Z_{i\omega\mp\frac{\varkappa}{2}}(\lambda\rho) = 0.\tag{2.12}$$

Multiplying by  $\chi_{\eta}^{(\pm)\dagger}(\mathbf{k})$  and summing over  $\eta$  we get

$$\sum_{\varkappa=\pm 1}\sum_{\eta}\chi_{\eta}^{(+)\dagger}(\mathbf{k})\left[1 + i\delta^{(J)}\left(\varkappa\gamma^{(0)} + \gamma^{(1)}\right)\right]\chi_{\eta}^{(\pm)}(\mathbf{k})Z_{i\omega\mp\frac{\varkappa}{2}}(\lambda\rho) = 0,\tag{2.13}$$

where the relation

$$\chi_{\eta'}^{(\pm)\dagger}(\mathbf{k})\gamma^{(0)}\gamma^{(1)}\chi_{\eta}^{(\pm)}(\mathbf{k}) = 0,\tag{2.14}$$

has been used. This relation follows from (2.9). The further simplification of (2.13) is done by using the relations

$$\begin{aligned}\sum_{\eta}\chi_{\eta}^{(j)\dagger}(\mathbf{k})\chi_{\eta}^{(j)}(\mathbf{k}) &= \frac{N}{2}, \\ \sum_{\eta}\chi_{\eta}^{(j)\dagger}(\mathbf{k})\left(\varkappa\gamma^{(0)} + \gamma^{(1)}\right)\chi_{\eta}^{(j)}(\mathbf{k}) &= \frac{imN}{2\lambda},\end{aligned}\tag{2.15}$$

with the result

$$Z_{i\omega-\frac{1}{2}}(\lambda\rho) + Z_{i\omega+\frac{1}{2}}(\lambda\rho) = 0,\tag{2.16}$$

for both positive and negative energy modes.

The mode functions (2.3) are normalized by the condition

$$\int d^Dx\sqrt{|g|}\bar{\psi}_{\sigma'}^{(\pm)}\gamma^0\psi_{\sigma}^{(\pm)} = \delta_{\sigma\sigma'},\tag{2.17}$$

where  $g$  is the determinant of the metric tensor. Here,  $\delta_{\sigma\sigma'}$  is understood as Dirac delta function for continuous quantum numbers and as Kronecker symbol for discrete ones.

We have described the features of the modes which are the same for the RR and RL regions. In the further consideration one needs to specify the region.

### 2.3 Mode functions in the RR region

In the RR region, the function  $I_{i\omega-\frac{1}{2}\gamma^{(0)}\gamma^{(1)}}(\lambda\rho)$  exponentially increases for large  $\rho$  and for normalizable modes we should take  $C_{1\sigma} = 0$ . The mode functions are expressed as

$$\psi_{\sigma}^{(j)} = N_{\sigma}^{\text{RR}} e^{-j i \omega \tau + i \mathbf{k} \cdot \mathbf{x}} K_{i\omega-j\frac{1}{2}\gamma^{(0)}\gamma^{(1)}}(\lambda\rho) \chi_{\eta}^{(j)}(\mathbf{k}), \quad (2.18)$$

with  $j = +, -$ . For the  $\rho$ -dependent part we have the relations

$$\begin{aligned} \left[ K_{i\omega \mp \frac{1}{2}\gamma^{(0)}\gamma^{(1)}}(\lambda\rho) \right]^{\dagger} &= K_{i\omega \pm \frac{1}{2}\gamma^{(0)}\gamma^{(1)}}(\lambda\rho), \\ \gamma^{(0)} K_{i\omega \mp \frac{1}{2}\gamma^{(0)}\gamma^{(1)}}(\lambda\rho) &= K_{i\omega \pm \frac{1}{2}\gamma^{(0)}\gamma^{(1)}}(\lambda\rho) \gamma^{(0)}. \end{aligned} \quad (2.19)$$

The eigenvalues of the quantum number  $\omega$  are determined by the equation (see (2.16))

$$K_{i\omega-\frac{1}{2}}(\lambda\rho_0) + K_{i\omega+\frac{1}{2}}(\lambda\rho_0) = 0. \quad (2.20)$$

Note that this equation can also be written in the form  $\text{Re}[K_{i\omega+\frac{1}{2}}(\lambda\rho_0)] = 0$ . We will denote the roots of the equation (2.20) for a given  $\lambda$  by  $\omega = \omega_n = \omega_n(\lambda)$ ,  $n = 1, 2, \dots$ . By taking into account that  $K_{i\omega_n \pm 1/2}(\lambda\rho_0) = \pm K_{i\omega_n + 1/2}(\lambda\rho_0)$ , we get

$$K_{i\omega_n \mp \frac{1}{2}\gamma^{(0)}\gamma^{(1)}}(\lambda\rho_0) = \pm \gamma^{(0)} \gamma^{(1)} K_{i\omega_n - \frac{1}{2}}(\lambda\rho_0). \quad (2.21)$$

The normalization condition (2.17) for the modes (2.18) is written in the form

$$J_{\eta\eta', nn'}^{(\text{RR})} |N_{\sigma}^{\text{RR}}|^2 = \frac{\delta_{nn'} \delta_{\eta\eta'}}{(2\pi)^{D-1}}, \quad (2.22)$$

where

$$J_{\eta\eta', nn'}^{(\text{RR})} = \chi_{\eta'}^{(+)\dagger}(\mathbf{k}) \int_{\rho_0}^{\infty} d\rho K_{i\omega_{n'} + \frac{1}{2}\gamma^{(0)}\gamma^{(1)}}(\lambda\rho) K_{i\omega_n - \frac{1}{2}\gamma^{(0)}\gamma^{(1)}}(\lambda\rho) \chi_{\eta}^{(+)}(\mathbf{k}). \quad (2.23)$$

The coefficient of  $|N_{\sigma}^{\text{RR}}|^2$  is expressed in terms of  $J_{\omega\omega'}$ , defined by (A.1), with  $\omega = \omega_n$ ,  $\omega' = \omega_{n'}$ ,  $\rho_1 \rightarrow \rho_0$ ,  $\rho_2 = \infty$ , and  $Z_{\nu}(x) = K_{\nu}(x)$ . This gives

$$J_{\eta\eta', nn'}^{(\text{RR})} = \frac{\delta_{\eta\eta'}}{2i} \lim_{\rho \rightarrow \rho_0} \rho \sum_{\varkappa = \pm 1} \frac{\varkappa K_{i\omega_n - \varkappa/2}(\lambda\rho) K_{i\omega_{n'} + \varkappa/2}(\lambda\rho)}{\omega' - \omega}. \quad (2.24)$$

For  $n' \neq n$ , we directly put  $\rho = \rho_0$  in the arguments of the Macdonald function and from the boundary condition it follows that, as expected,  $\sum_{\varkappa = \pm 1} \varkappa K_{i\omega_n - \varkappa/2}(\lambda\rho) K_{i\omega_{n'} + \varkappa/2}(\lambda\rho) = 0$ . In the limit  $\omega' \rightarrow \omega$ , we evaluate the right-hand side of (2.24) by using the L'Hôpital's rule. By taking into account that  $\varkappa K_{i\omega_n - \varkappa/2}(\lambda\rho_0) = -K_{i\omega_n + 1/2}(\lambda\rho_0)$ , we get

$$J_{\eta\eta', nn}^{(\text{RR})} = \delta_{\eta\eta'} \frac{i}{2} \rho_0 K_{i\omega_n + 1/2}(\lambda\rho_0) \partial_{\omega} \bar{K}_{i\omega + 1/2}(\lambda\rho_0) |_{\omega = \omega_n}, \quad (2.25)$$

with the notation

$$\bar{K}_{i\omega + 1/2}(z) = K_{i\omega + 1/2}(z) + K_{i\omega - 1/2}(z). \quad (2.26)$$

From the Wronskian for the modified Bessel functions, by taking into account that  $K_{i\omega_n - 1/2}(\lambda\rho_0) = -K_{i\omega_n + 1/2}(\lambda\rho_0)$ , one finds

$$K_{i\omega_n + \frac{1}{2}}(\lambda\rho_0) = -\frac{1}{\lambda\rho_0 \bar{K}_{i\omega_n + 1/2}(\lambda\rho_0)}, \quad (2.27)$$

where

$$\bar{I}_{i\omega+1/2}(z) = I_{i\omega+1/2}(z) - I_{i\omega-1/2}(z). \quad (2.28)$$

The final expression for  $J_{\eta\eta',nn'}^{(\text{RR})}$  reads

$$J_{\eta\eta',nn'}^{(\text{RR})} = \delta_{\eta\eta'} \delta_{nn'} \frac{\partial_\omega \bar{K}_{i\omega+1/2}(\lambda\rho_0)}{2i\lambda \bar{I}_{i\omega+1/2}(\lambda\rho_0)} \Big|_{\omega=\omega_n}. \quad (2.29)$$

With this result, the normalization coefficient is obtained from (2.22):

$$|N_\sigma^{\text{RR}}|^2 = \frac{2i\lambda \bar{I}_{i\omega+1/2}(\lambda\rho_0)}{(2\pi)^{D-1} \partial_\omega \bar{K}_{i\omega+1/2}(\lambda\rho_0)} \Big|_{\omega=\omega_n}. \quad (2.30)$$

Note that  $\bar{K}_{-i\omega+1/2}(z) = \bar{K}_{i\omega+1/2}(z)$  and, hence, the function  $\bar{K}_{i\omega+1/2}(z)$  is real for real values of  $\omega$  and  $z$ . In addition, we have  $K_{1/2-i\omega_n}(\lambda\rho_0) = -K_{1/2+i\omega_n}(\lambda\rho_0)$  and the function  $K_{1/2+i\omega_n}(\lambda\rho_0)$  is purely imaginary. From (2.27) it follows that the same is the case for the function  $\bar{I}_{i\omega_n+1/2}(\lambda\rho_0)$  and the function  $i\bar{I}_{i\omega_n+1/2}(\lambda\rho_0)$  in (2.30) is real.

## 2.4 Mode functions in the RL region

In the RL region, corresponding to  $0 < \rho < \rho_0$ , both the functions  $I_\nu(x)$  and  $K_\nu(x)$  are allowed in (2.4). The relative coefficient in the linear combination of those functions is determined by the boundary condition (2.16). The mode functions are presented in the form

$$\psi_\sigma^{(j)} = N_\sigma^{\text{RL}} e^{-j\omega\tau + i\mathbf{k}\cdot\mathbf{x}} Z_{i\omega-j\frac{1}{2}\gamma^{(0)}\gamma^{(1)}}(\lambda\rho) \chi_\eta^{(j)}(\mathbf{k}), \quad (2.31)$$

where

$$Z_\nu(\lambda\rho) = e^{-\nu\pi i} I_\nu(\lambda\rho) + C_\sigma K_\nu(\lambda\rho). \quad (2.32)$$

Note that the function  $Z_\nu(\lambda\rho)$  obeys the same recurrence relations as the function  $K_\nu(\lambda\rho)$  (the factor  $e^{-\nu\pi i}$  in front of  $I_\nu(\lambda\rho)$  is added for this purpose). The coefficient  $C_\sigma$  is found from the boundary condition (2.16) and is given by the expression

$$C_\sigma = ie^{\pi\omega} \frac{\bar{I}_{i\omega+1/2}(\lambda\rho_0)}{\bar{K}_{i\omega+1/2}(\lambda\rho_0)}, \quad (2.33)$$

with the notations (2.26) and (2.28). Note that unlike the RR region, the spectrum of  $\omega$  in the RL region is continuous. It can be shown that

$$C_\sigma^* = C_\sigma + \frac{i}{\pi} (e^{2\pi\omega} + 1), \quad (2.34)$$

where the star stands for the complex conjugate.

By using the relation (2.34) we can see that (compare with (2.19))

$$\begin{aligned} \left[ Z_{i\omega \mp \frac{1}{2}\gamma^{(0)}\gamma^{(1)}}(\lambda\rho) \right]^\dagger &= Z_{i\omega \pm \frac{1}{2}\gamma^{(0)}\gamma^{(1)}}(\lambda\rho), \\ \gamma^{(0)} Z_{i\omega \mp \frac{1}{2}\gamma^{(0)}\gamma^{(1)}}(\lambda\rho) &= Z_{i\omega \pm \frac{1}{2}\gamma^{(0)}\gamma^{(1)}}(\lambda\rho) \gamma^{(0)}, \end{aligned} \quad (2.35)$$

and the normalization condition for the positive energy modes (2.31) is written in the form

$$J_{\eta\eta',\omega\omega'}^{(\text{RL})} |N_\sigma^{\text{RL}}|^2 = \frac{\delta(\omega - \omega')}{(2\pi)^{D-1}} \delta_{\eta\eta'}, \quad (2.36)$$

where

$$J_{\eta\eta',\omega\omega'}^{(\text{RL})} = \chi_{\eta'}^{(+)\dagger}(\mathbf{k}) \int_0^{\rho_0} d\rho Z_{i\omega'+\frac{1}{2}\gamma^{(0)}\gamma^{(1)}}(\lambda\rho) Z_{i\omega-\frac{1}{2}\gamma^{(0)}\gamma^{(1)}}(\lambda\rho) \chi_{\eta}^{(+)}(\mathbf{k}). \quad (2.37)$$

By using the result (A.9) with  $\rho_2 \rightarrow \rho_0$ ,  $\rho_1 \rightarrow 0$ , and the boundary condition (2.16), we can see that the contribution from the upper limit  $\rho = \rho_0$  becomes zero. The expression (2.37) is transformed to

$$J_{\eta\eta',\omega\omega'}^{(\text{RL})} = \frac{\delta_{\eta\eta'}}{2i\lambda} \lim_{x \rightarrow 0} x \sum_{\varkappa=\pm 1} \frac{\varkappa Z_{i\omega-\varkappa/2}(x) Z_{i\omega'+\varkappa/2}(x)}{\omega' - \omega}, \quad (2.38)$$

where we have introduced  $x = \lambda\rho$ . By making use of the asymptotics for the modified Bessel functions for small values of the argument and the relation (2.34), we can see that for  $0 < x \ll 1$ , to the leading order,

$$\sum_{\varkappa=\pm 1} \varkappa Z_{i\omega-\varkappa/2}(x) Z_{i\omega'+\varkappa/2}(x) \approx i\pi |C_\sigma|^2 \frac{\sin[(\omega - \omega') \ln(x/2)]}{x \cosh(\omega\pi)}. \quad (2.39)$$

Plugging this in (2.38) and by taking into account that

$$\lim_{x \rightarrow 0} \frac{\sin(u \ln(x/2))}{u} = -\pi \delta(u), \quad (2.40)$$

we get

$$J_{\eta\eta',\omega\omega'}^{(\text{RL})} = \frac{\delta_{\eta\eta'} \pi^2 |C_\sigma|^2}{2\lambda \cosh(\omega\pi)} \delta(\omega' - \omega). \quad (2.41)$$

With this result, the normalization constant in the RL region is found to be

$$|N_\sigma^{\text{RL}}|^2 = \frac{8\lambda \cosh(\omega\pi)}{(2\pi)^{D+1} |C_\sigma|^2}, \quad (2.42)$$

with  $C_\sigma$  given by (2.33).

### 3 Fermion condensate

After specifying the normalized mode functions in the RR and RL regions, we investigate the VEVs of physical observables. In this section, we consider the fermion condensate. The formation of a nonzero fermion condensate is critically important in quantum field theory and in many condensed matter systems exhibiting superconductivity and superfluidity. The condensate provides a mechanism that gives fermions mass and acts as an order parameter for dynamical symmetry breaking, such as chiral symmetry breaking in quantum chromodynamics through the formation of a quark condensate. In the context of the Nambu-Jona-Lasinio model with quartic interaction, the effective dynamical mass of fermions is proportional to the fermion condensate, and the coefficient is determined by the four-fermion coupling constant.

The fermion condensate is defined as the VEV  $\langle 0 | \bar{\psi}\psi | 0 \rangle \equiv \langle \bar{\psi}\psi \rangle$ , where  $|0\rangle$  stands for the Fulling-Rindler vacuum state. Expanding the field operator in terms of complete set of modes  $\{\psi_\sigma^{(+)}, \psi_\sigma^{(-)}\}$ , the condensate is presented in the form of the mode-sum

$$\langle \bar{\psi}\psi \rangle = \frac{1}{2} \sum_\sigma \left( \bar{\psi}_\sigma^{(-)} \psi_\sigma^{(-)} - \bar{\psi}_\sigma^{(+)} \psi_\sigma^{(+)} \right), \quad (3.1)$$

where  $\sum_\sigma$  includes a summation over discrete quantum numbers and an integration over the continuous ones. The fermion condensate in the RR and RL regions will be studied separately.

### 3.1 Condensate in the RR region

Plugging the mode functions (2.18) in (3.1) and using the second relation in (2.15), the fermion condensate in the RR-region is presented in the form

$$\langle \bar{\psi}\psi \rangle = -\frac{mN}{2^D \pi^{D-1}} \int d\mathbf{k} \sum_{n=1}^{\infty} \frac{\bar{I}_{i\omega+1/2}(\lambda\rho_0)}{\partial_{\omega} \bar{K}_{i\omega+1/2}(\lambda\rho_0)} \left[ K_{i\omega+\frac{1}{2}}^2(\lambda\rho) - K_{i\omega-\frac{1}{2}}^2(\lambda\rho) \right]_{\omega=\omega_n}. \quad (3.2)$$

This expression is divergent and some regularization scheme is implicitly assumed (e.g., point-splitting or a cutoff function). For points  $\rho \neq \rho_0$ , the divergences are the same as those in a problem without boundaries and the renormalization of the condensate reduces to the corresponding procedure in the problem without boundaries. This can also be understood based on general considerations. In quantum field theories in curved spaces, the divergences of vacuum averages at a given spacetime point are uniquely determined by the local geometric characteristics of the background spacetime at that point, such as the Riemann tensor and combinations constructed from it. Introducing boundaries does not change the local geometry of spacetime at points outside the boundary; therefore, it does not lead to new divergences in the local physical characteristics of vacuum averages. Thus, renormalizing these averages is equivalent to renormalizing them in a problem without boundaries. In the problem under consideration, the background spacetime is flat, and subtracting the Minkowski spacetime parts from the vacuum expectation values of local observables yields finite physical values at points outside the boundary.

The above arguments do not apply to points on the boundary. Typically, local vacuum expectation values diverge as they approach the boundary. In the literature on the Casimir effect, these divergences are studied for various boundary and background geometries (see, for example, [11]-[14]). The presence of surface divergences indicates that physical quantities containing contributions from local averages at boundary points necessitate additional renormalization. An important example of such a quantity is the total vacuum energy. In the following discussion we will explicitly separate the boundary-free contributions in local observables such as the fermion condensate and the mean energy-momentum tensor. The corresponding renormalization procedure has already been discussed in [32]. Thus, the choice of a specific regularization scheme is not important for the subsequent analysis.

From the point of view of further calculations, the representation (3.2) has two disadvantages: (i) the eigenvalues  $\omega_n$  of the energy are given implicitly, as roots of the equation (2.20), and (ii) the series terms for large  $n$  are highly oscillatory. Both of these difficulties can be overcome by applying to the series over  $n$  in (3.2) the summation formula (B.5) with the function

$$F(z) = K_{iz+\frac{1}{2}}^2(\lambda\rho) - K_{iz-\frac{1}{2}}^2(\lambda\rho). \quad (3.3)$$

This allows to present the fermion condensate in the form

$$\langle \bar{\psi}\psi \rangle = \langle \bar{\psi}\psi \rangle_0 + \frac{mN}{(2\pi)^D} \int d\mathbf{k} \int_0^{\infty} dx \frac{\bar{I}_{x+1/2}(\lambda\rho_0)}{\bar{K}_{x+1/2}(\lambda\rho_0)} \left[ K_{x+\frac{1}{2}}^2(\lambda\rho) - K_{x-\frac{1}{2}}^2(\lambda\rho) \right], \quad (3.4)$$

where

$$\langle \bar{\psi}\psi \rangle_0 = \frac{4mN}{(2\pi)^{D+1}} \int d\mathbf{k} \int_0^{\infty} d\omega \cosh \pi\omega \operatorname{Im} \left[ K_{\frac{1}{2}-i\omega}^2(\lambda\rho) \right]. \quad (3.5)$$

The part  $\langle \bar{\psi}\psi \rangle_0$  comes from the integral in the square brackets of (B.5) and coincides with the fermion condensate in the boundary-free geometry. The representation (3.4) is well-adapted for investigating the properties of the condensate. First, explicit knowledge of the eigenmodes  $\omega_n$  is not required. Second, the integrand monotonically decreases within the range of the integration variables near the upper limits of integration. Third, the boundary-induced contribution is explicitly separated.

The renormalization of (3.5) is done by subtracting the condensate in Minkowski spacetime:  $\langle \bar{\psi}\psi \rangle_0^{\text{ren}} = \langle \bar{\psi}\psi \rangle_0 - \langle \bar{\psi}\psi \rangle_{\text{M}}$  and the renormalized fermion condensate for the Fulling-Rindler vacuum in the absence of boundaries is expressed as [32]

$$\langle \bar{\psi}\psi \rangle_0^{\text{ren}} = \frac{2^{1-D} m N}{\pi^{\frac{D+3}{2}} \Gamma\left(\frac{D-1}{2}\right)} \int_0^\infty d\omega e^{-\pi\omega} \int_m^\infty d\lambda \lambda (\lambda^2 - m^2)^{\frac{D-3}{2}} \text{Im} \left[ K_{1/2-i\omega}^2(\lambda\rho) \right], \quad (3.6)$$

for  $D \geq 2$ . For  $D = 1$  we have

$$\langle \bar{\psi}\psi \rangle_0^{\text{ren}} = \frac{m}{\pi^2} \int_0^\infty d\omega e^{-\pi\omega} \text{Im} \left[ K_{1/2-i\omega}^2(m\rho) \right]. \quad (3.7)$$

Another representation for the boundary-free part in the fermion condensate is provided in [32]:

$$\langle \bar{\psi}\psi \rangle_0^{\text{ren}} = -\frac{2Nm^D}{(2\pi)^{\frac{D+3}{2}}} \int_0^\infty du \frac{u \sinh u}{u^2 + \pi^2/4} f_{\frac{D-1}{2}}(2m\rho \cosh u), \quad (3.8)$$

with the function

$$f_\nu(z) = z^{-\nu} K_\nu(z). \quad (3.9)$$

The expression (3.8) shows that for a massive field the boundary-free part in the fermion condensate is negative.

Integrating the boundary-induced contribution in (3.4) over the angular coordinates of the momentum  $\mathbf{k}$ , the renormalized fermion condensate in the RR region is decomposed as

$$\langle \bar{\psi}\psi \rangle_{\text{ren}} = \langle \bar{\psi}\psi \rangle_0^{\text{ren}} + \langle \bar{\psi}\psi \rangle_{\text{b}}, \quad (3.10)$$

where the boundary-induced contribution is given by the formula

$$\begin{aligned} \langle \bar{\psi}\psi \rangle_{\text{b}} &= \frac{2^{1-D} m N}{\pi^{\frac{D+1}{2}} \Gamma\left(\frac{D-1}{2}\right)} \int_m^\infty d\lambda \lambda (\lambda^2 - m^2)^{\frac{D-3}{2}} \\ &\times \int_{1/2}^\infty d\nu \frac{\bar{I}_\nu(\lambda\rho_0)}{\bar{K}_\nu(\lambda\rho_0)} [K_\nu^2(\lambda\rho) - K_{\nu-1}^2(\lambda\rho)], \end{aligned} \quad (3.11)$$

for  $D \geq 2$ . In the case  $D = 1$ , the boundary-induced part is expressed as

$$\langle \bar{\psi}\psi \rangle_{\text{b}} = \frac{m}{\pi} \int_{1/2}^\infty d\nu \frac{\bar{I}_\nu(m\rho_0)}{\bar{K}_\nu(m\rho_0)} [K_\nu^2(m\rho) - K_{\nu-1}^2(m\rho)]. \quad (3.12)$$

In the integration range of (3.11) we have the relations

$$\bar{I}_\nu(z) < 0, \quad \bar{K}_\nu(z) > 0, \quad K_\nu(z) > K_{\nu-1}(z). \quad (3.13)$$

We conclude from this that, in the RR region, both the boundary-free and boundary-induced contributions to the fermion condensate are negative for a massive field. In the zero-mass limit, the condensate tends to zero like  $\langle \bar{\psi}\psi \rangle_{\text{b}} \propto m$  for  $D > 2$  and like  $\langle \bar{\psi}\psi \rangle_{\text{b}} \propto m \ln m$  for  $D = 2$ . In the case  $D = 1$ , the condensate tends to nonzero limiting value. Taking the limit  $m \rightarrow 0$  in (3.12), we obtain

$$\langle \bar{\psi}\psi \rangle_{\text{b}} |_{m=0} = -\frac{1}{2\pi\rho \ln(\rho/\rho_0)}, \quad D = 1. \quad (3.14)$$

Let us consider the asymptotics of the fermion condensate near the plate and at large distances from it. Near the boundary, assuming that  $\rho/\rho_0 - 1 \ll 1$ , the dominant contribution to (3.11) comes from

large values of  $\lambda$  and  $\nu$ . Introducing a new integration variable  $z = \lambda/\nu$ , we use the uniform asymptotic expansions of the modified Bessel functions for large values of the order (see, for example, [53]). It can be seen that for  $\nu \gg 1$ , to the leading order,

$$\begin{aligned} \frac{\bar{I}_\nu(\nu u)}{\bar{K}_\nu(\nu u)} &\approx \frac{e^{2\nu\eta(u)}}{\pi u} (u - t_u) (t_u + 1), \\ K_\nu^2(\nu u) - K_{\nu-1}^2(\nu u) &\approx \frac{\pi e^{-2\nu\eta(u)}}{\nu u^2} \left(1 - \frac{1}{t_u}\right) \end{aligned} \quad (3.15)$$

where

$$\eta(u) = t_u + \ln \frac{u}{1 + t_u}, \quad t_u = \sqrt{1 + u^2}. \quad (3.16)$$

Substituting these asymptotics in (3.11) and by taking into account that for  $\rho/\rho_0 - 1 \ll 1$  one has  $\eta(u\rho/\rho_0) - \eta(u) \approx t_u(\rho/\rho_0 - 1)$ , for the leading term in the expansion of the fermion condensate over the distance from the boundary we get

$$\langle \bar{\psi}\psi \rangle_b \approx \frac{(4\pi)^{-\frac{D+1}{2}} mN}{(\rho - \rho_0)^{D-1}} \left[ \Gamma\left(\frac{D-1}{2}\right) - \frac{\Gamma\left(\frac{D}{2} - 1\right)}{\Gamma\left(\frac{D-1}{2}\right)} \Gamma\left(\frac{D}{2}\right) \right], \quad (3.17)$$

for  $D \geq 3$ . For  $D = 2$  the asymptotic is given by

$$\langle \bar{\psi}\psi \rangle_b \approx \frac{\sqrt{m}}{4\pi (\rho - \rho_0)^{3/2}} \left[ \frac{\Gamma\left(\frac{3}{4}\right)}{\Gamma\left(\frac{1}{4}\right)} - \frac{\Gamma\left(\frac{5}{4}\right)}{\Gamma\left(\frac{3}{4}\right)} \right]. \quad (3.18)$$

In the case  $D = 1$  one obtains

$$\langle \bar{\psi}\psi \rangle_b \approx -\frac{1}{2\pi (\rho - \rho_0)}. \quad (3.19)$$

This leading term does not depend on the mass and could also be obtained directly from (3.14).

At large distances from the boundary and for a massive field,  $m\rho \gg 1$ , the argument  $\lambda\rho$  of the Macdonald functions in (3.12) is large and we use the corresponding asymptotic [53]. The dominant contribution to the integral over  $\lambda$  comes from the region near the lower limit of the integral. In the leading order for  $D \geq 1$  one obtains

$$\langle \bar{\psi}\psi \rangle_b \approx \frac{Nm^D e^{-2m\rho}}{2^{D+1} \pi^{\frac{D-1}{2}} (m\rho)^{\frac{D+3}{2}}} \int_{1/2}^{\infty} d\nu (2\nu - 1) \frac{\bar{I}_\nu(m\rho_0)}{\bar{K}_\nu(m\rho_0)}. \quad (3.20)$$

The asymptotic of the boundary-free part in the limit  $m\rho \gg 1$  reads

$$\langle \bar{\psi}\psi \rangle_0^{\text{ren}} \approx -\frac{Nm^D e^{-2m\rho}}{2^{D+1} \pi^{\frac{D+5}{2}} (m\rho)^{\frac{D+3}{2}}}. \quad (3.21)$$

For the ratio of the boundary-induced and boundary-free contributions we get

$$\frac{\langle \bar{\psi}\psi \rangle_b}{\langle \bar{\psi}\psi \rangle_0^{\text{ren}}} \approx -\pi^3 \int_{1/2}^{\infty} d\nu (2\nu - 1) \frac{\bar{I}_\nu(m\rho_0)}{\bar{K}_\nu(m\rho_0)}. \quad (3.22)$$

This ratio does not depend on the number of spatial dimensions. The numerical evaluation shows that the right-hand side in (3.22) is smaller than 1 for  $m\rho_0 < 0.04$  and larger than 1 for  $m\rho_0 > 0.04$ . For  $m\rho_0 = 1$  the ratio (3.22) is near 40 and it increases with increasing  $m\rho_0$ . Hence, in the range  $m\rho_0 > 0.04$ , the total VEV at large distances is dominated by the boundary-induced part. For a massless field the fermion condensate vanishes in spatial dimensions  $D \geq 2$  and the large-distance asymptotic for  $D = 1$  is given by (3.14).

### 3.2 Condensate in the RL region

With the mode functions (2.31), the fermion condensate in the RL-region is expressed by the formula

$$\langle \bar{\psi}\psi \rangle = \frac{2imN}{(2\pi)^{D+1}} \int_0^\infty d\omega \int d\mathbf{k} \frac{\cosh(\omega\pi)}{|C_\sigma|^2} \left[ Z_{i\omega+\frac{1}{2}}^2(\lambda\rho) - Z_{i\omega-\frac{1}{2}}^2(\lambda\rho) \right], \quad (3.23)$$

where  $C_\sigma$  is defined in (2.33) and

$$Z_{i\omega\pm\frac{1}{2}}(\lambda\rho) = C_\sigma K_{i\omega\pm\frac{1}{2}}(\lambda\rho) \mp e^{\pi\omega} i I_{i\omega\pm\frac{1}{2}}(\lambda\rho). \quad (3.24)$$

It is easy to see that

$$Z_{i\omega\pm\frac{1}{2}}(\lambda\rho) = \left[ Z_{i\omega\mp\frac{1}{2}}(\lambda\rho) \right]^*, \quad (3.25)$$

and the expression in the right-hand side of (3.23) is explicitly real. In order to separate the boundary-free contribution we use the identity

$$\sum_{\kappa=\pm 1} \kappa \frac{Z_{i\omega+\frac{\kappa}{2}}^2(\lambda\rho)}{|C_\sigma|^2} = \sum_{\kappa=\pm 1} \kappa \left[ K_{i\omega+\frac{\kappa}{2}}^2(\lambda\rho) + \frac{\pi \bar{K}_{i\omega+\frac{1}{2}}(\lambda\rho_0)}{2 \cosh(\omega\pi)} \sum_{j=\pm 1} \frac{j I_{j i\omega+\frac{\kappa}{2}}^2(\lambda\rho)}{\bar{I}_{j i\omega+\frac{1}{2}}(\lambda\rho_0)} \right]. \quad (3.26)$$

The proof of this relation is presented in Appendix C. The identity (3.26) allows to write the fermion condensate (3.23) in the form

$$\langle \bar{\psi}\psi \rangle = \langle \bar{\psi}\psi \rangle_0 + \frac{imN}{2(2\pi)^D} \int d\mathbf{k} \sum_{\kappa, j=\pm 1} \kappa j \int_0^\infty d\omega \frac{\bar{K}_{j i\omega+\frac{1}{2}}(\lambda\rho_0)}{\bar{I}_{j i\omega+\frac{1}{2}}(\lambda\rho_0)} I_{j i\omega+\frac{\kappa}{2}}^2(\lambda\rho), \quad (3.27)$$

with the boundary-free condensate  $\langle \bar{\psi}\psi \rangle_0$  given by (3.5).

For the further transformation of the boundary-induced part in (3.27), we rotate the integration contour over  $\omega$  by the angle  $\pi/2$  for the term  $j = -1$  and by the angle  $-\pi/2$  for the term  $j = 1$ . For the integrals we get

$$\int_0^\infty d\omega \frac{\bar{K}_{j i\omega+\frac{1}{2}}(\lambda\rho_0)}{\bar{I}_{j i\omega+\frac{1}{2}}(\lambda\rho_0)} I_{j i\omega+\frac{\kappa}{2}}^2(\lambda\rho) = -j i \int_0^\infty dx \frac{\bar{K}_{x+\frac{1}{2}}(\lambda\rho_0)}{\bar{I}_{x+\frac{1}{2}}(\lambda\rho_0)} I_{x+\frac{\kappa}{2}}^2(\lambda\rho), \quad (3.28)$$

and the fermion condensate is presented as

$$\langle \bar{\psi}\psi \rangle = \langle \bar{\psi}\psi \rangle_0 + \frac{mN}{(2\pi)^D} \int d\mathbf{k} \int_0^\infty dx \frac{\bar{K}_{x+1/2}(\lambda\rho_0)}{\bar{I}_{x+1/2}(\lambda\rho_0)} \left[ I_{x+\frac{1}{2}}^2(\lambda\rho) - I_{x-\frac{1}{2}}^2(\lambda\rho) \right]. \quad (3.29)$$

For  $D \geq 2$ , integrating over the angular part of the momentum, the condensate is decomposed as (3.10), where the boundary-induced contribution is given by the expression

$$\begin{aligned} \langle \bar{\psi}\psi \rangle_b &= \frac{2^{1-D} mN}{\pi^{\frac{D+1}{2}} \Gamma(\frac{D-1}{2})} \int_m^\infty d\lambda \lambda (\lambda^2 - m^2)^{\frac{D-3}{2}} \\ &\times \int_{1/2}^\infty d\nu \frac{\bar{K}_\nu(\lambda\rho_0)}{\bar{I}_\nu(\lambda\rho_0)} \left[ I_\nu^2(\lambda\rho) - I_{\nu-1}^2(\lambda\rho) \right]. \end{aligned} \quad (3.30)$$

The renormalized boundary-free condensate is expressed by the formula (3.6). In the case  $D = 1$  we get

$$\langle \bar{\psi}\psi \rangle_b = \frac{m}{\pi} \int_{1/2}^\infty d\nu \frac{\bar{K}_\nu(m\rho_0)}{\bar{I}_\nu(m\rho_0)} \left[ I_\nu^2(m\rho) - I_{\nu-1}^2(m\rho) \right]. \quad (3.31)$$

By taking into account the relations (3.13) and  $I_\nu(z) < I_{\nu-1}(z)$ , it is seen that the boundary-induced contribution in the fermion condensate is positive in the RL region. For a massless field the fermion condensate vanishes in spatial dimensions  $D \geq 2$  and is given by

$$\langle \bar{\psi}\psi \rangle_b = \frac{1}{2\pi\rho \ln(\rho_0/\rho)}, \quad (3.32)$$

for  $D = 1$ . Comparing with (3.14), we see that in this special case the expressions for the condensates in the RL and RR regions differ by the sign.

The asymptotic near the boundary is found in the way similar to that we have used for the RR-region, by using the uniform asymptotic expansions of the modified Bessel functions. By taking into account (3.15) and

$$I_\nu^2(\nu u) - I_{\nu-1}^2(\nu u) \approx -\frac{e^{2\nu\eta(u)}}{\pi\nu u^2} \left(1 + \frac{1}{t_u}\right), \quad (3.33)$$

we can show that in the leading order

$$\langle \bar{\psi}\psi \rangle_b \approx \frac{(4\pi)^{-\frac{D+1}{2}} mN}{(\rho_0 - \rho)^{D-1}} \left[ \Gamma\left(\frac{D-1}{2}\right) + \frac{\Gamma\left(\frac{D}{2}-1\right)}{\Gamma\left(\frac{D-1}{2}\right)} \Gamma\left(\frac{D}{2}\right) \right], \quad (3.34)$$

for  $D \geq 3$ . In the case  $D = 2$  one has

$$\langle \bar{\psi}\psi \rangle_b \approx \frac{\sqrt{m}}{4\pi(\rho_0 - \rho)^{3/2}} \left[ \frac{\Gamma\left(\frac{5}{4}\right)}{\Gamma\left(\frac{3}{4}\right)} + \frac{\Gamma\left(\frac{3}{4}\right)}{\Gamma\left(\frac{1}{4}\right)} \right], \quad (3.35)$$

and for  $D = 1$  we get

$$\langle \bar{\psi}\psi \rangle_b \approx \frac{1}{2\pi(\rho_0 - \rho)}. \quad (3.36)$$

In Fig. 2, we present the total fermion condensate (3.10), in units of  $1/\rho_0^D$ , as a function of the ratio  $\rho/\rho_0$  (left panel) and of the mass (right panel) for spatial dimension  $D = 3$ . On the left panel, the graphs for the RR and RL regions are plotted for  $m\rho_0 = 0.5$  and the dashed curve corresponds to the fermion condensate in the boundary-free problem (given by (3.8)). The numbers near the curves on the right panel correspond to the values of the ratio  $\rho/\rho_0$ . As already concluded based on asymptotic analysis, the fermion condensate is dominated by the boundary-induced part near the mirror and by the boundary-free contribution near the Rindler horizon.

From the asymptotic analysis presented above, it follows that for the taken value of the combination  $m\rho_0$ , the contribution imposed by the boundary dominates over the entire range  $\rho_0 < \rho < \infty$ . The boundary-free contribution dominates only in the region close to the horizon. An important feature of the fermion condensate in the RL region is that it changes sign at a certain value of acceleration. In models with interacting fields, changing the sign of the fermion condensate can have important consequences. They include tachyonic instabilities and spontaneous symmetry breaking in models with interacting scalar and fermionic fields and phase transition in Nambu-Jona-Lasinio-type models with quartic fermionic interactions.

## 4 VEV of the energy-momentum tensor

In this section, we will consider another important local characteristic of the vacuum state: the VEV of the energy-momentum tensor,  $\langle 0|T_{\mu\alpha}|0\rangle \equiv \langle T_{\mu\alpha} \rangle$ . In addition to describing the distribution of the

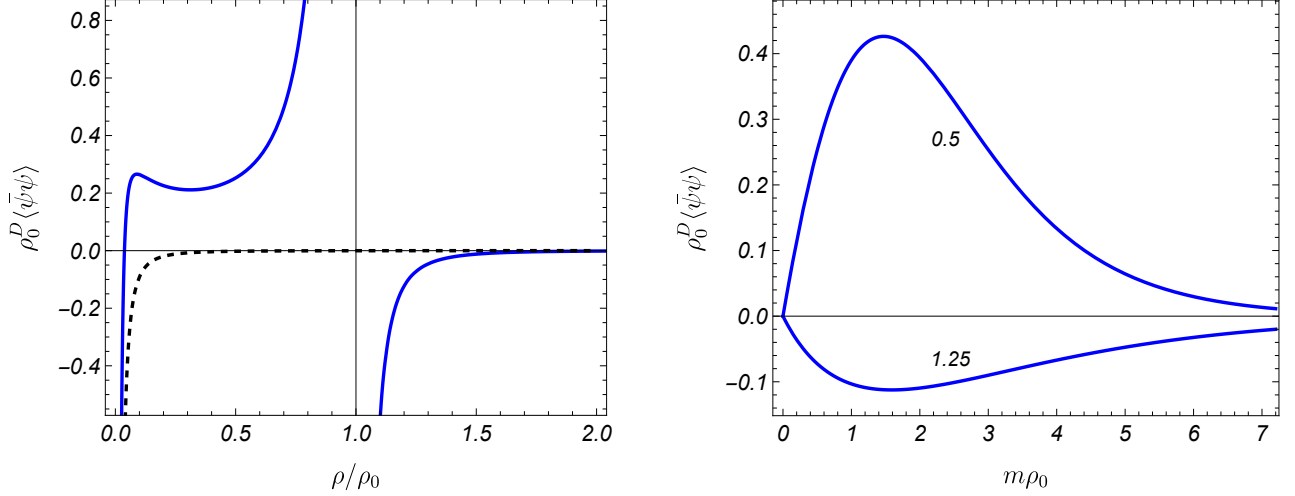


Figure 2: The fermion condensate for spatial dimension  $D = 3$  in the RR and RL regions versus  $\rho/\rho_0$  (left panel) and  $m\rho_0$  (right panel). The graphs on the left panel are plotted for  $m\rho_0 = 0.5$  and the dashed curve presents the condensate in the boundary-free geometry. The numbers near the curves on the right panel present the values of  $\rho/\rho_0$ .

vacuum energy density and stresses, it acts as a source of the gravitational field in the semiclassical Einstein equations. The corresponding mode-sum formula reads

$$\langle T_{\mu\alpha} \rangle = -\frac{i}{4} \sum_{\sigma} \sum_{j=+,-} j [\bar{\psi}_{\sigma}^{(j)}(x) \gamma_{(\mu} \nabla_{\alpha)} \psi_{\sigma}^{(j)}(x) - (\nabla_{(\mu} \bar{\psi}_{\sigma}^{(j)}(x)) \gamma_{\alpha)} \psi_{\sigma}^{(j)}(x)], \quad (4.1)$$

where the brackets denote symmetrization over the enclosed indices and

$$\nabla_{\mu} \bar{\psi}_{\sigma}^{(j)} = \partial_{\mu} \bar{\psi}_{\sigma}^{(j)} - \bar{\psi}_{\sigma}^{(j)} \Gamma_{\mu}. \quad (4.2)$$

In both RR and RL regions the vacuum energy-momentum tensor is diagonal. From the problem symmetry we also expect that

$$\langle T_2^2 \rangle = \langle T_3^3 \rangle = \dots = \langle T_D^D \rangle. \quad (4.3)$$

Of course, these relations are checked by direct evaluation.

#### 4.1 RR region

By using the mode functions (2.18) and the relations for the spinors  $\chi_{\eta}^{(j)}(\mathbf{k})$  given above, the diagonal components of the vacuum energy-momentum tensor in the RR region are presented in the form (no summation over  $\mu$ )

$$\langle T_{\mu}^{\mu} \rangle = -\frac{N}{2^D \pi^{D-1}} \int d\mathbf{k} \sum_{n=1}^{\infty} \frac{\bar{I}_{i\omega+\frac{1}{2}}(\lambda\rho_0)}{\partial_{\omega} \bar{K}_{i\omega+\frac{1}{2}}(\lambda\rho_0)} F_{\mu} [K_{i\omega+\frac{1}{2}}(\lambda\rho)]|_{\omega=\omega_n}. \quad (4.4)$$

Here, for a given function  $G_{\nu}(z)$ , the notations

$$\begin{aligned} F_0 [G_{\nu}(\lambda\rho)] &= \delta_G \frac{\lambda}{\rho} (2\nu - 1) G_{\nu}(\lambda\rho) G_{\nu-1}(\lambda\rho), \\ F_1 [G_{\nu}(\lambda\rho)] &= \delta_G \lambda^2 [G'_{\nu}(\lambda\rho) G_{\nu-1}(\lambda\rho) - G_{\nu}(\lambda\rho) G'_{\nu-1}(\lambda\rho)], \\ F_l [G_{\nu}(\lambda\rho)] &= \frac{\lambda^2 - m^2}{D-1} [G_{\nu-1}^2(\lambda\rho) - G_{\nu}^2(\lambda\rho)], \end{aligned} \quad (4.5)$$

with  $l = 2, 3, \dots, D$ , are introduced and the prime stands for the derivative with respect to the argument of the function. In the discussion below, as a function  $G_\nu(z)$  we will take the functions  $K_\nu(z)$ ,  $Z_\nu(z)$ , and  $I_\nu(z)$ . For those functions we define

$$\delta_G = \begin{cases} 1, & G = K, Z \\ -1, & G = I \end{cases}. \quad (4.6)$$

The function  $F_{l,i\omega}[G_{x+1/2}(\lambda\rho)]$  for the components  $\langle T_l^l \rangle$ , with  $l = 2, 3, \dots, D$ , obtained by the direct evaluation from (4.1) has the form  $(k^l)^2 [G_{x-1/2}^2(\lambda\rho) - G_{x+1/2}^2(\lambda\rho)]$ . We have replaced  $(k^l)^2$  by  $(\lambda^2 - m^2)/(D-1)$  by taking into account the relations (4.3). In deriving the expression for those components, we have employed the relation

$$\sum_\eta \chi_\eta^{(j)\dagger} \left( \gamma^{(0)} \pm \gamma^{(1)} \right) \gamma^{(l)} \chi_\eta^{(j)}(\mathbf{k}) = \pm \frac{iN}{2\lambda} k^l. \quad (4.7)$$

By using the recurrence formulas for the modified Bessel functions, it can be seen that the relation

$$F_1[G_\nu(\lambda\rho)] = \frac{1-D}{1-m^2/\lambda^2} F_2[G_\nu(\lambda\rho)] - F_0[G_\nu(\lambda\rho)] \quad (4.8)$$

holds between the functions (4.5).

For the series over  $n$  in (4.4) we use the summation formula (B.5). The part in the VEV coming from the integral in the square brackets of (B.5) corresponds to the VEV of the energy-momentum tensor in the boundary-free problem. Denoting it by  $\langle T_\mu^\mu \rangle_0$ , the VEV is decomposed as (no summation over  $\mu$ )

$$\langle T_\mu^\mu \rangle = \langle T_\mu^\mu \rangle_0 + N \int \frac{d\mathbf{k}}{(2\pi)^D} \int_0^\infty dx \frac{\bar{I}_{x+\frac{1}{2}}(\lambda\rho_0)}{\bar{K}_{x+\frac{1}{2}}(\lambda\rho_0)} F_\mu[K_{x+\frac{1}{2}}(\lambda\rho)], \quad (4.9)$$

with

$$\langle T_\mu^\mu \rangle_0 = \frac{2iN}{(2\pi)^{D+1}} \int d\mathbf{k} \int_0^\infty d\omega \cosh(\pi\omega) F_\mu[K_{i\omega+\frac{1}{2}}(\lambda\rho)]. \quad (4.10)$$

For points away from the boundary, the renormalization is reduced to the renormalization of (4.10). Similar to the fermion condensate, that is done by subtracting the VEV of the energy-momentum tensor for the Minkowski vacuum:  $\langle T_\mu^\alpha \rangle_0^{\text{ren}} = \langle T_\mu^\alpha \rangle_0 - \langle T_\mu^\alpha \rangle_{\text{M}}$ . The renormalized VEV takes the form (no summation over  $\mu$ ) [32]

$$\langle T_\mu^\mu \rangle_0^{\text{ren}} = \frac{2^{-D} iN}{\pi^{\frac{D+3}{2}} \Gamma(\frac{D-1}{2})} \int_0^\infty d\omega e^{-\pi\omega} \int_m^\infty d\lambda \lambda (\lambda^2 - m^2)^{\frac{D-3}{2}} F_\mu[K_{i\omega+\frac{1}{2}}(\lambda\rho)], \quad (4.11)$$

for  $D \geq 2$ . After integration over the angular coordinates of  $\mathbf{k}$  in (4.9), the renormalized VEV in the RR region is presented in the decomposed form (no summation over  $\mu$ )

$$\langle T_\mu^\mu \rangle_{\text{ren}} = \langle T_\mu^\mu \rangle_0^{\text{ren}} + \langle T_\mu^\mu \rangle_{\text{b}}, \quad (4.12)$$

with the boundary-induced part

$$\langle T_\mu^\mu \rangle_{\text{b}} = \frac{2^{1-D} N}{\pi^{\frac{D+1}{2}} \Gamma(\frac{D-1}{2})} \int_m^\infty d\lambda \lambda (\lambda^2 - m^2)^{\frac{D-3}{2}} \int_{1/2}^\infty d\nu \frac{\bar{I}_\nu(\lambda\rho_0)}{\bar{K}_\nu(\lambda\rho_0)} F_\mu[K_\nu(\lambda\rho)]. \quad (4.13)$$

In the special case  $D = 1$  one has (no summation over  $\mu$ )

$$\langle T_\mu^\mu \rangle_{\text{b}} = \frac{1}{\pi} \int_{1/2}^\infty d\nu \frac{\bar{I}_\nu(m\rho_0)}{\bar{K}_\nu(m\rho_0)} F_\mu[K_\nu(m\rho)], \quad (4.14)$$

and

$$\langle T_\mu^\mu \rangle_0^{\text{ren}} = \frac{i}{2\pi^2} \int_0^\infty d\omega e^{-\pi\omega} F_\mu[K_{i\omega+\frac{1}{2}}(m\rho)], \quad (4.15)$$

with  $\mu = 0, 1$ , and in the expressions (4.5)  $\lambda$  is replaced by  $m$ . Simpler representation for the boundary-free VEV is given in [32] (no summation over  $l$ ):

$$\begin{aligned} \langle T_0^0 \rangle_0^{\text{ren}} &= -\frac{2Nm^{D+1}}{(2\pi)^{\frac{D+3}{2}}} \int_0^\infty du \frac{u \sinh u}{u^2 + \pi^2/4} \left[ f_{\frac{D-1}{2}}(2m\rho \cosh u) + D f_{\frac{D+1}{2}}(2m\rho \cosh u) \right], \\ \langle T_l^l \rangle_0^{\text{ren}} &= \frac{2Nm^{D+1}}{(2\pi)^{\frac{D+3}{2}}} \int_0^\infty du \frac{u \sinh u}{u^2 + \pi^2/4} f_{\frac{D+1}{2}}(2m\rho \cosh u), \end{aligned} \quad (4.16)$$

with  $l = 1, 2, \dots, D$ , and the function  $f_\nu(x)$  is defined by (3.9). This shows that the vacuum stresses are isotropic in the boundary-free problem. The vacuum effective pressure along the  $l$ th direction is given by  $p_l^{(0)} = -\langle T_l^l \rangle_0^{\text{ren}}$ . As seen from (4.16), in the boundary-free problem both the energy density and the pressure in the Fulling-Rindler vacuum are negative.

We can check that the VEV of the energy-momentum tensor obeys the continuity equation  $\nabla_\alpha \langle T_\mu^\alpha \rangle_{\text{ren}} = 0$ . For the problem under consideration it is reduced to the relation  $\langle T_0^0 \rangle_{\text{ren}} = \partial_\rho (\rho \langle T_1^1 \rangle_{\text{ren}})$ . By using the differential equation for the function  $K_\nu(z)$  it is easily seen that  $\partial_\rho (\rho F_1[K_\nu(\lambda\rho)]) = F_0[K_\nu(\lambda\rho)]$  and, hence, the continuity equation indeed takes place. In addition, for the functions  $F_\mu[K_{x+1/2}(\lambda\rho)]$  we have

$$\sum_{\mu=0}^D F_\mu[K_{x+\frac{1}{2}}(\lambda\rho)] = m^2 \left[ K_{x+\frac{1}{2}}^2(\lambda\rho) - K_{x-\frac{1}{2}}^2(\lambda\rho) \right]. \quad (4.17)$$

From here it follows that the VEV of the energy-momentum tensor obeys the trace relation

$$\langle T_\mu^\mu \rangle_{\text{ren}} = m \langle \bar{\psi}\psi \rangle_{\text{ren}}. \quad (4.18)$$

Comparing the expressions for the fermion condensate and the parallel stresses, we can check that the following relation takes place (no summation over  $l = 2, 3, \dots, D$ )

$$\langle T_l^l \rangle_0^{\text{ren}} = -\frac{\pi}{m} \langle \bar{\psi}\psi \rangle_{(D+3),0}^{\text{ren}}, \quad \langle T_l^l \rangle_{\text{b}} = -\frac{\pi}{m} \langle \bar{\psi}\psi \rangle_{(D+3),\text{b}}, \quad (4.19)$$

where  $\langle \bar{\psi}\psi \rangle_{(D+3),0}^{\text{ren}}$  and  $\langle \bar{\psi}\psi \rangle_{(D+3),\text{b}}$  are the fermion condensates in  $(D+3)$ -dimensional Rindler spacetime, given by (3.8) and (4.16) with the replacements  $D \rightarrow D+2$  (note that  $N_{D+3} = 2N_{D+1}$ ).

For a massless fermionic field the vacuum energy-momentum tensor is traceless. In this special case the boundary-induced energy-momentum tensor is simplified to (no summation over  $\mu$ )

$$\langle T_\mu^\mu \rangle_{\text{b}} = \frac{N(2\rho)^{1-D}}{\pi^{\frac{D+1}{2}} \Gamma(\frac{D-1}{2})} \int_0^\infty du u^{D-2} \int_{1/2}^\infty d\nu \frac{\bar{I}_\nu(u\rho_0/\rho)}{\bar{K}_\nu(u\rho_0/\rho)} F_\mu[K_\nu(u)], \quad (4.20)$$

where the functions  $F_\mu[K_\nu(u)]$  are given by (4.5) with  $G = K$ ,  $m = 0$ , and  $\lambda = u/\rho$ . In (4.20), an additional factor  $1/\rho^2$  comes from the functions  $F_\mu[K_\nu(u)]$  and the combination  $\rho^{D+1} \langle T_\mu^\mu \rangle_{\text{b}}$  is a function of only the ratio  $\rho_0/\rho$ . The boundary-free contribution is expressed as [32] (no summation over  $l$ )

$$\langle T_l^l \rangle_0^{\text{ren}} = -\frac{1}{D} \langle T_0^0 \rangle_0^{\text{ren}} = \frac{2N\Gamma(\frac{D+1}{2})}{(4\pi)^{\frac{D+3}{2}} \rho^{D+1}} \int_0^\infty du \frac{u \sinh u}{\left(u^2 + \frac{\pi^2}{4}\right) \cosh^{D+1} u}, \quad (4.21)$$

with  $l = 1, 2, \dots, D$ .

From the relations (3.13) it follows that the boundary-induced contribution in the vacuum energy density is negative and the corresponding stresses  $\langle T_l^l \rangle_b$ ,  $l = 2, 3, \dots, D$ , are positive in the RR region:

$$\langle T_0^0 \rangle_b < 0, \langle T_2^2 \rangle_b > 0, \rho > \rho_0. \quad (4.22)$$

Note that the same inequalities take place for the boundary-free parts (4.16).

Now, let us consider the asymptotic behavior of the components of the energy-momentum tensor in the RR region. In the way similar to that we have used for the fermion condensate, it can be shown that for points near the boundary,  $\rho/\rho_0 - 1 \ll 1$ , the leading term of the boundary-induced mean energy density is expressed as

$$\langle T_0^0 \rangle_b \approx \frac{(D-1)N}{2(4\pi)^{\frac{D+1}{2}}(\rho-\rho_0)^{D+1}} \left[ \Gamma\left(\frac{D+1}{2}\right) - \frac{\Gamma\left(\frac{D}{2}\right)}{\Gamma\left(\frac{D+1}{2}\right)} \Gamma\left(\frac{D}{2}+1\right) \right]. \quad (4.23)$$

For the normal and parallel stresses one gets (no summation over  $l = 2, 3, \dots, D$ )

$$\langle T_1^1 \rangle_b \approx -\frac{\rho/\rho_0 - 1}{D} \langle T_0^0 \rangle_b, \quad \langle T_l^l \rangle_b \approx -\frac{\langle T_0^0 \rangle_b}{D-1}. \quad (4.24)$$

As seen, near the boundary we have  $|\langle T_1^1 \rangle_b| \ll |\langle T_0^0 \rangle_b|$ . In the region under consideration the total VEV is dominated by the boundary-induced part.

The large-distance asymptotic of the boundary-induced energy-momentum tensor for a massive field, assuming  $m\rho \gg 1$ , is given by (no summation over  $l = 1, 2, \dots, D$ )

$$\langle T_0^0 \rangle_b \approx -2m\rho \langle T_l^l \rangle_b \approx \frac{Nm^{D+1}e^{-2m\rho}}{2^{D+1}\pi^{\frac{D-1}{2}}(m\rho)^{\frac{D+3}{2}}} \int_{1/2}^{\infty} d\nu (2\nu-1) \frac{\bar{I}_\nu(m\rho_0)}{\bar{K}_\nu(m\rho_0)}, \quad (4.25)$$

with an exponential decay. Note that one has  $\langle T_0^0 \rangle_b \approx m \langle \bar{\psi}\psi \rangle_b$ . The behavior of the boundary-free contribution in the same limit is described by

$$\langle T_l^l \rangle_0^{\text{ren}} \approx -\frac{\langle T_0^0 \rangle_0^{\text{ren}}}{2m\rho} \approx \frac{Nm^{D+1}e^{-2m\rho}}{2^{D+2}(\pi m\rho)^{\frac{D+5}{2}}}. \quad (4.26)$$

Both the contributions to the energy density are suppressed by the same factor  $(m\rho)^{-\frac{D+3}{2}} e^{-2m\rho}$ . In the leading order, the vacuum stresses are isotropic and, compared to the energy density, they contain an additional suppression factor  $1/(m\rho)$ . The relative contributions of the boundary-induced and boundary-free parts in the energy density for the region  $m\rho \gg 1$  is given by the right-hand side of (3.22). In the region  $m\rho_0 > 0.04$  and for  $m\rho \gg 1$ , boundary-induced part dominates in the total VEV of the energy-momentum tensor. For a massless field and  $\rho \gg \rho_0$ , the leading terms of the asymptotic expansion are expressed as (no summation over  $l = 1, 2, \dots, D$ )

$$\langle T_l^l \rangle_b \approx -\frac{1}{D} \langle T_0^0 \rangle_b \approx \frac{N\Gamma\left(\frac{D}{2}\right) \ln^{-2}(2\rho/\rho_0)}{2^{D+1}\pi^{\frac{D}{2}+1} D \rho^{D+1}}. \quad (4.27)$$

The boundary-free part for a massless field is given by (4.21) and it decays like  $1/\rho^{D+1}$ . This shows that for a massless field the boundary-free part dominates at large distances.

## 4.2 RL region

By the evaluation similar to that for the RR region, the VEV of the energy-momentum tensor in the RL region is presented in the form (no summation over  $\mu$ )

$$\langle T_\mu^\mu \rangle = \frac{2iN}{(2\pi)^{D+1}} \int d\mathbf{k} \int_0^\infty d\omega \frac{\cosh(\omega\rho)}{|C_\sigma|^2} F_\mu[Z_{i\omega+\frac{1}{2}}(\lambda\rho)], \quad (4.28)$$

where the functions  $F_\mu[Z_\nu(\lambda\rho)]$  are defined by (4.5) with the replacement  $G \rightarrow Z$ . The boundary-induced contribution in the VEV (4.28) is obtained by subtracting the boundary free part  $\langle T_\mu^\mu \rangle_0$ , given by (4.10). The VEV is expressed as (no summation over  $\mu$ )

$$\langle T_\mu^\mu \rangle = \langle T_\mu^\mu \rangle_0 + \frac{2iN}{(2\pi)^{D+1}} \int d\mathbf{k} \int_0^\infty d\omega \cosh(\omega\pi) \left\{ \frac{F_\mu[Z_{i\omega+\frac{1}{2}}(\lambda\rho)]}{|C_\sigma|^2} - F_\mu[K_{i\omega+\frac{1}{2}}(\lambda\rho)] \right\}. \quad (4.29)$$

By using the identities given in Appendix C, for the difference in the integrand we have

$$\frac{F_\mu[Z_\nu(\lambda\rho)]}{|C_\sigma|^2} - F_\mu[K_\nu(\lambda\rho)] = \sum_{j=\pm 1} \frac{j\pi \bar{K}_\nu(\lambda\rho_0) F_\mu \left[ I_{j i\omega+\frac{1}{2}}(\lambda\rho) \right]}{2 \cosh(\omega\pi) \bar{I}_{j i\omega+1/2}(\lambda\rho_0)}, \quad (4.30)$$

where  $\nu = i\omega + 1/2$ . Substituting this in (4.29), we rotate the integration contour over  $\omega$  in the complex  $\omega$ -plane by the angle  $-\pi/2$  for the term with  $j = +1$  and by the angle  $\pi/2$  for the part with  $j = -1$ . This leads to the following representation (no summation over  $\mu$ ):

$$\langle T_\mu^\mu \rangle = \langle T_\mu^\mu \rangle_0 + \frac{N}{(2\pi)^D} \int d\mathbf{k} \int_0^\infty dx \frac{\bar{K}_{x+1/2}(\lambda\rho_0)}{\bar{I}_{x+1/2}(\lambda\rho_0)} F_\mu \left[ I_{x+\frac{1}{2}}(\lambda\rho) \right]. \quad (4.31)$$

The renormalized VEV is obtained by subtracting the VEV for the Minkowski vacuum. The subtraction is reduced to the renormalization of the boundary-free part and for  $D \geq 2$  we get the decomposition (4.12) with the boundary-induced contribution (no summation over  $\mu$ )

$$\langle T_\mu^\mu \rangle_b = \frac{2^{1-D} N}{\pi^{\frac{D+1}{2}} \Gamma\left(\frac{D-1}{2}\right)} \int_m^\infty d\lambda \lambda (\lambda^2 - m^2)^{\frac{D-3}{2}} \int_{1/2}^\infty d\nu \frac{\bar{K}_\nu(\lambda\rho_0)}{\bar{I}_\nu(\lambda\rho_0)} F_\mu [I_\nu(\lambda\rho)], \quad (4.32)$$

where the functions  $F_\mu[I_\nu(\lambda\rho)]$  are defined in (4.5) with  $G = I$  and with  $\delta_I = -1$ . In the special case  $D = 1$  we get

$$\langle T_\mu^\mu \rangle_b = \frac{1}{\pi} \int_{1/2}^\infty d\nu \frac{\bar{I}_\nu(m\rho_0)}{\bar{K}_\nu(m\rho_0)} F_\mu [I_\nu(m\rho)]. \quad (4.33)$$

From the relations (3.13) we see that the boundary-induced energy density is positive and the stresses  $\langle T_l^l \rangle_b$ ,  $l = 2, 3, \dots, D$ , are negative in the RL region:

$$\langle T_0^0 \rangle_b > 0, \quad \langle T_2^2 \rangle_b < 0, \quad \rho < \rho_0. \quad (4.34)$$

These signs are opposite to those for the boundary-free contributions. Similar to the RR region, we have the relations (4.19) between the normal stress in  $(D+1)$ -dimensional spacetime and the fermion condensate in  $(D+3)$ -dimensional spacetime. The expression (4.32) is further simplified for a massless field (no summation over  $\mu$ ):

$$\langle T_\mu^\mu \rangle_b = \frac{N (2\rho)^{1-D}}{\pi^{\frac{D+1}{2}} \Gamma\left(\frac{D-1}{2}\right)} \int_0^\infty du u^{D-2} \int_{1/2}^\infty d\nu \frac{\bar{K}_\nu(u\rho_0/\rho)}{\bar{I}_\nu(u\rho_0/\rho)} F_\mu [I_\nu(u)], \quad (4.35)$$

with the function  $F_\mu [I_\nu(u)]$  from (3.13), where  $G = I$  and  $\lambda = u/\rho$ .

Near the boundary we use the uniform asymptotic expansions for the modified Bessel functions. The calculations similar to those for the RR region lead to the result

$$\langle T_0^0 \rangle_b \approx \frac{(4\pi)^{-\frac{D+1}{2}} (D-1) N}{2(\rho_0 - \rho)^{D+1}} \left[ \Gamma\left(\frac{D+1}{2}\right) + \frac{\Gamma\left(\frac{D}{2}\right)}{\Gamma\left(\frac{D+1}{2}\right)} \Gamma\left(\frac{D}{2} + 1\right) \right], \quad (4.36)$$

for the boundary-induced energy density. The asymptotics for other components are related to the energy density by the formulas (4.24). Figure 3 displays the dependence of the vacuum energy density (in units of  $1/\rho_0^{D+1}$ ) on the ratio  $\rho/\rho_0$  (left panel) and on  $m\rho_0$  (right panel). The graphs are plotted for the spatial dimension  $D = 3$  and for  $m\rho_0 = 0.5$  on the left panel. The dashed curve on the left panel corresponds to the vacuum energy density in the geometry without boundaries. The numbers near the curves on the right panel correspond to the values of the ratio  $\rho/\rho_0$ . In accordance with the asymptotic analysis given above, near the horizon the vacuum energy density is dominated by the boundary-free contribution and is negative. In the region near the boundary, the energy density is dominated by the boundary-induced contribution and it is positive in the RL region and negative in the RR region.

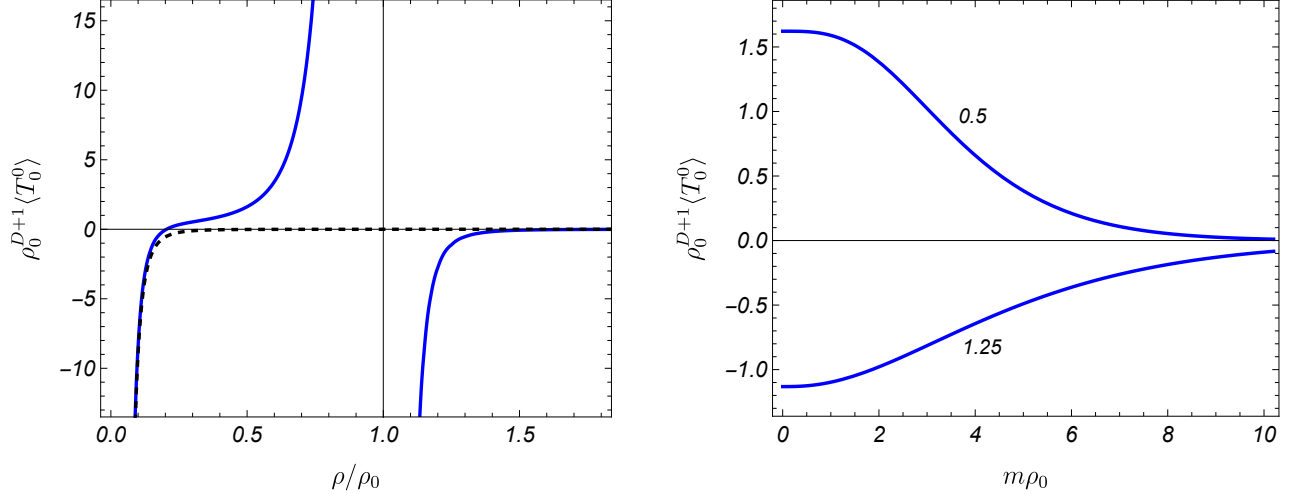


Figure 3: The energy density in the Fulling-Rindler vacuum for the  $D = 3$  Dirac field as a function of  $\rho/\rho_0$  (left panel) and  $m\rho_0$  (right panel). For the graphs on the left panel we have taken  $m\rho_0 = 0.5$  and the numbers near the curves on the right panel correspond to the values of  $\rho/\rho_0$ . The dashed curve on the left panel presents the energy density in the boundary-free problem.

In Fig. 4 we have plotted the vacuum stresses along the directions perpendicular and parallel to the boundary as functions of  $\rho/\rho_0$  (left panel) and  $m\rho_0$  (right panel). The full and dashed curves correspond to the stresses  $\langle T_1^1 \rangle$  and  $\langle T_2^2 \rangle$  in the model with  $D = 3$ . For the graphs on the left panel  $m\rho_0 = 0.5$  and the numbers near the curves on the right panel present the values of the ratio  $\rho/\rho_0$ . The vacuum stresses in the boundary-free problem are presented by the dot-dashed curve (recall that in the boundary-free geometry  $\langle T_1^1 \rangle = \langle T_2^2 \rangle$ ).

It is of interest to compare the results for the Fulling-Rindler vacuum with the vacuum expectation values for a planar mirror, with bag boundary condition, at rest relative to an inertial observer in the Minkowski vacuum. The corresponding VEVs were investigated in Ref. [54] for a more general geometry involving two parallel plates and with toroidal compactification of a part of spatial dimensions (see also [55, 56] for the Casimir energy and the vacuum current density). The results for a single boundary in Minkowski spacetime are obtained as a special case. In this case, of course, the VEVs are symmetric with respect to the plate. The background line element reads  $ds_M^2 = \eta_{\mu\nu} dx^\mu dx^\nu$ , with  $-\infty < x^\mu < +\infty$ , and assuming that the boundary is located at  $x'^1 = 0$ , for the fermion condensate from [54] we obtain

$$\langle \bar{\psi}\psi \rangle_{\text{ren}}^{(M)} = \frac{Nm^D}{(2\pi)^{\frac{D+1}{2}}} \left[ f_{\frac{D-1}{2}}(2m|x'^1|) - 2m|x'^1| f_{\frac{D+1}{2}}(2m|x'^1|) \right], \quad (4.37)$$

where  $f_\nu(x)$  is defined by (3.9). The condensate given by (4.37) is negative. For the VEV of the energy-momentum tensor, after integration of the corresponding expressions in [54], one gets (no summation

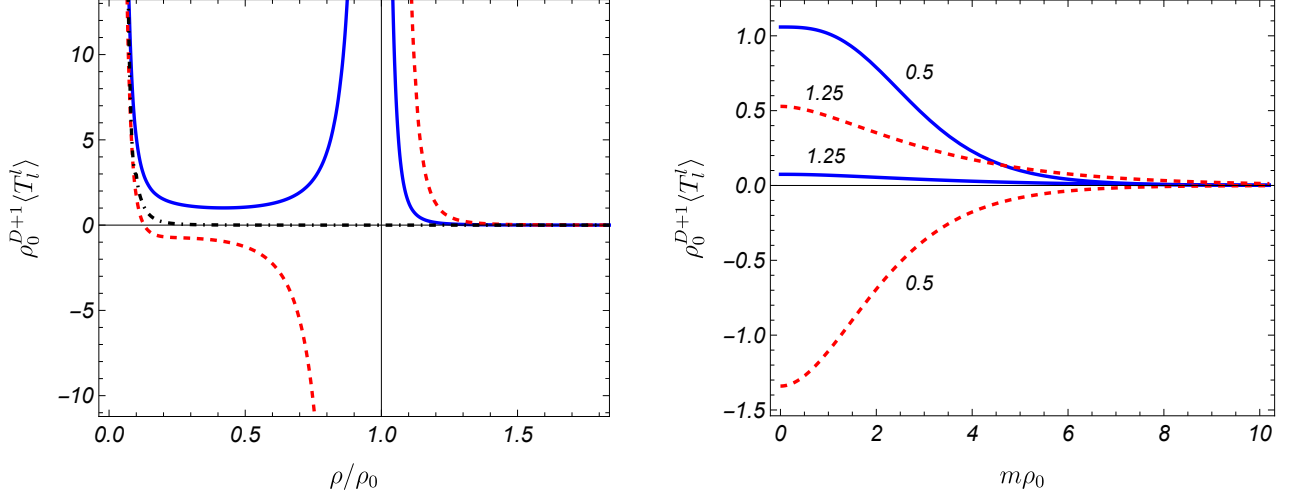


Figure 4: The same as in Fig. 3 for the stresses parallel and perpendicular to the boundary (full and dashed curves, respectively). The dot-dashed curve on the left panel corresponds to the stress in the boundary-free problem.

over  $\mu$ )  $\langle T_\mu^\mu \rangle_{\text{ren}}^{(M)} = m \langle \bar{\psi}\psi \rangle_{\text{ren}}^{(M)} / D$ , for  $\mu = 0, 2, \dots, D$ , and  $\langle T_1^1 \rangle_{\text{ren}}^{(M)} = 0$ . These results could be obtained from general arguments: from the covariant conservation equation  $\partial \langle T_\mu^\alpha \rangle_{\text{ren}}^{(M)} / \partial x'^\alpha = 0$  and from the trace relation  $\langle T_\mu^\mu \rangle_{\text{ren}}^{(M)} = m \langle \bar{\psi}\psi \rangle_{\text{ren}}^{(M)}$ . The effects of a brane with bag boundary condition and cosmic string on the Dirac vacuum in background of (4+1)-dimensional anti-de Sitter spacetime were studied in [57]. It can be checked that the result (4.37) for  $D = 4$  is obtained from the corresponding formula in Ref. [57] in the flat spacetime limit and in the absence of a cosmic string. For a massless field, from (4.37) we get

$$\langle \bar{\psi}\psi \rangle_{\text{ren}}^{(M)} = -\frac{N\Gamma\left(\frac{D+1}{2}\right)}{(4\pi)^{\frac{D+1}{2}} |x'^1|^D}, \quad m = 0, \quad (4.38)$$

and the VEV of the energy-momentum tensor vanishes  $\langle T_\mu^\nu \rangle_{\text{ren}}^{(M)} = 0$ . Comparing with the results obtained above for the Fulling-Rindler vacuum, we see that the situation here is significantly different from the case of a boundary uniformly accelerating through the Fulling-Rindler vacuum. In the latter case, the fermion condensate vanishes for a massless field in spatial dimensions  $D \geq 2$ , while the VEV of the energy-momentum tensor is nonzero.

The above calculation of the VEVs does not use a specific representation of the Dirac matrices  $\gamma^{(b)}$ . In particular, this means that the results obtained for the fermion condensate and the vacuum energy-momentum tensor apply to both types of Dirac fields that realize two inequivalent irreducible representations of the Clifford algebra in an odd number of spacetime dimensions ( $D$  being an even number). 2D Dirac materials are among the interesting condensed matter realizations of the Dirac model in spatial dimension  $D = 2$ . The long-wavelength dynamics of the electronic subsystem in such materials (the most famous example of which is graphene) is described by the Dirac equation, in which the Fermi velocity of the electrons is used instead of the speed of light (see, e.g., [58, 59, 60]). An effective Rindler metric for the corresponding quasiparticles can be generated by engineering the strain profile in graphene (see, for example, [61, 62, 63] and references therein). The setup we discussed can be used to model and investigate edge-induced effects in these 2D structures within the framework of effective Dirac theory.

## 5 Fermionic Casimir densities in gravitational fields

In this section, we will apply the above results to the study of boundary-imposed contributions to the local characteristics of the fermionic vacuum in gravitational fields. The cases of weak gravitational fields and background geometries that are conformally related to Rindler spacetime will be discussed.

### 5.1 Weak gravitational fields

For a weakly gravitating system of a mass  $M$ , the line element in a  $(D + 1)$ -dimensional spacetime is approximated by (see, for example, [64])

$$ds_g^2 \approx [1 - w(r')] dt'^2 - \left[1 + \frac{w(r')}{D-2}\right] \sum_{i=1}^D (dx'^i)^2, \quad (5.1)$$

in the coordinates  $x'^\mu$ . Here,  $w(r') = (r_g/r')^{D-2} \ll 1$ ,  $r'^2 = \sum_{i=1}^D (x'^i)^2$ , and

$$r_g^{D-2} = \frac{16\pi GM}{(D-1)\Omega_{D-1}}, \quad (5.2)$$

with  $\Omega_{D-1} = 2\pi^{D/2}/\Gamma(D/2)$  being the area of a unit  $(D - 1)$ -sphere. The acceleration at a given point is expressed as

$$g(r') = \frac{D/2 - 1}{r'} w(r'). \quad (5.3)$$

Directing the local axis  $x'^1$  along the radial direction and expanding the metric around  $r' = r'_0$  one gets

$$ds_g^2 \approx (1 - w_0 + 2g_0 x'^1) dt'^2 - \left(1 + \frac{w_0 - 2g_0 x'^1}{D-2}\right) \sum_{i=1}^D (dx'^i)^2, \quad (5.4)$$

where  $w_0 = w(r'_0)$  and  $g_0 = g(r'_0)$ . In the next step, we make a transition to a new coordinate system  $(t, z, \mathbf{x})$ , with  $\mathbf{x} = (x^2, \dots, x^D)$ , defined by the relations (for the transformation in the special case  $D = 3$  see also [49])

$$\begin{aligned} t' &= \frac{t}{\sqrt{1 - w_0}}, \quad x'^1 = \frac{z + \frac{g_0(z^2 - \mathbf{x}^2)}{2(D-2)}}{\sqrt{1 + \frac{w_0}{D-2}}}, \\ x'^i &= \frac{1 + \frac{g_0 z}{D-2}}{\sqrt{1 + \frac{w_0}{D-2}}} x^i, \quad i \geq 2. \end{aligned} \quad (5.5)$$

This brings the line element to the form

$$ds_g^2 \approx (1 + g_0 z)^2 dt^2 - dz^2 - d\mathbf{x}^2. \quad (5.6)$$

Introducing the coordinates  $(\tau, \rho)$  according to  $\tau = g_0 t$  and  $\rho = z + 1/g_0$ , the line element is written in the Rindler form (1.2).

Having the VEVs in the Rindler spacetime, the corresponding VEVs for a boundary in the geometry (5.1) are found by a coordinate transformation  $(\tau, \rho, \mathbf{x}) \rightarrow (t', x'^1, \mathbf{x}')$ . We denote these VEVs by  $\langle \bar{\psi} \psi \rangle'$  and  $\langle T_\nu^\mu \rangle'$  for the fermion condensate and vacuum energy-momentum tensor. The fermion condensate is a scalar and one gets  $\langle \bar{\psi} \psi \rangle' = \langle \bar{\psi} \psi \rangle$ . The VEV of the energy-momentum tensor is obtained by using the standard law for the transformation of second rank tensors (no summation over  $\mu$ ):

$$\langle T_\mu^\mu \rangle' = \langle T_\mu^\mu \rangle, \quad \langle T_l^1 \rangle' = \frac{g_0 x'^l}{D-2} (\langle T_1^1 \rangle - \langle T_2^2 \rangle), \quad l = 2, \dots, D. \quad (5.7)$$

In the absence of boundaries, the vacuum stresses are isotropic,  $\langle T_1^1 \rangle_0^{\text{ren}} = \langle T_2^2 \rangle_0^{\text{ren}}$ , and the corresponding off-diagonal contribution in (5.7) vanishes. The appearance of the off-diagonal component is a purely boundary-induced effect.

## 5.2 Gravitational fields conformally related to the Rindler spacetime

With the results presented above, we can find the boundary induced VEVs for a massless Dirac field in the problems where the background geometry is conformally related to the Rindler spacetime. Under the conformal transformation  $\tilde{g}_{\mu\nu} = \Omega^2(x)g_{\mu\nu}$  of the metric tensor the Dirac matrices and the field transform as  $\tilde{\gamma}^\mu = \Omega^{-1}\gamma^\mu$  and  $\tilde{\psi} = \Omega^{-D/2}\psi$  and the Dirac equation for massless fields is conformally invariant. In the presence of boundaries, by taking into account that the normal to the boundary transforms as  $\tilde{n}_\mu = \Omega n_\mu$ , we conclude that the bag boundary condition is also invariant under conformal transformations. Consequently, by conformal transformation one can relate the boundary-induced VEVs in conformally connected problems. For a massless field, the fermion condensate becomes zero in spatial dimensions  $D \geq 2$  and we will focus on the VEV of the energy-momentum tensor.

Let us denote by  $\langle \tilde{T}_\mu^\nu \rangle$  the VEV of the energy-momentum tensor for a fermionic field in a spacetime with the metric tensor  $\tilde{g}_{\mu\nu}$  conformally related to the metric tensor defined by (1.2). We assume the presence of a boundary which is a conformal image of the boundary  $\rho = \rho_0$  in the problem on the Rindler bulk. The expectation value  $\langle \tilde{T}_\mu^\nu \rangle$  is decomposed into two contributions. The first one, denoted here as  $\langle \tilde{T}_\mu^\nu \rangle_G$ , is the geometrical part and is uniquely determined by the geometrical characteristics of the curved metric  $\tilde{g}_{\mu\nu}$ . The second contribution is conformally related to the VEV  $\langle T_\mu^\nu \rangle$  for the Fulling-Rindler vacuum and the total VEV is expressed as (see, for example, [1])

$$\langle \tilde{T}_\mu^\nu \rangle = \langle \tilde{T}_\mu^\nu \rangle_G + \frac{\langle T_\mu^\nu \rangle}{\Omega^{D+1}(x)}. \quad (5.8)$$

In this relation, it is assumed that the vacuum state in the problem with the metric tensor  $\tilde{g}_{\mu\nu}$  is the conformal counterpart of the Fulling-Rindler vacuum. A similar relation holds for the boundary-free parts,  $\langle \tilde{T}_\mu^\nu \rangle_0 = \langle \tilde{T}_\mu^\nu \rangle_G + \Omega^{-D-1} \langle T_\mu^\nu \rangle_0$ . Combining this with (5.8), we get the relation

$$\langle \tilde{T}_\mu^\nu \rangle_b = \frac{\langle T_\mu^\nu \rangle_b}{\Omega^{D+1}(x)} \quad (5.9)$$

for the boundary-induced VEVs.

As an example we consider a cosmological model with negative curvature spatial foliation (open universe). In conformal time  $\tau$  and spherical spatial coordinates  $(\chi, \theta_1, \theta_2, \dots, \theta_{D-1})$ , with  $0 \leq \theta_l \leq \pi$ ,  $l = 1, \dots, D-2$ ,  $0 \leq \theta_{D-1} \leq 2\pi$ , the line element is given by

$$d\tilde{s}^2 = a^2(\tau) (d\tau^2 - d\chi^2 - \sinh^2 \chi d\Omega_{D-1}^2), \quad (5.10)$$

where  $a(\tau)$  is the scale factor. The synchronous time coordinate  $t$  is defined by  $t = \int d\tau a(\tau)$ . In order to bring the Rindler line element (1.2) into the form conformal to (5.10), we make spatial coordinate transformation (see also [1] for the case  $D = 3$ )

$$\begin{aligned} \rho &= \alpha_0 (\cosh \chi - \sinh \chi \cos \theta_1)^{-1}, \\ x^i &= \rho \sinh \chi \cos \theta_i \prod_{n=1}^{i-1} \sin \theta_n, \quad x^D = \rho \sinh \chi \prod_{n=1}^{D-1} \sin \theta_n, \end{aligned} \quad (5.11)$$

with  $i = 2, \dots, D-1$  and  $\alpha_0$  being a constant. With this transformation, the line element becomes

$$ds_R^2 = \rho^2 (d\tau^2 - d\chi^2 - \sinh^2 \chi d\Omega_{D-1}^2). \quad (5.12)$$

From here, the conformal relation  $d\tilde{s}^2 = [a(\tau)/\rho]^2 ds_{\text{R}}^2$  is seen with the cosmological metric defined by (5.10). The conformal factor in (5.9) is given by  $\Omega(x) = a(\tau)/\rho$ .

In the relation (5.8) the left- and right-hand sides are written in the same coordinate system. Considering the coordinates  $(\tau, \chi, \theta_1, \theta_2, \dots, \theta_{D-1})$ , one needs to transform the energy-momentum tensor  $\langle T_{\mu}^{\nu} \rangle$  from Section 4 to this coordinate system. We will denote the transformed VEV by  $\langle \tilde{T}_{\mu}^{\nu} \rangle_{\text{R}}$ . By using the standard transformation law for the second rank tensors, the following expressions are obtained for the diagonal components (no summation over  $l$ ):

$$\begin{aligned} \langle \tilde{T}_l^l \rangle_{\text{R}} &= \langle T_l^l \rangle, \quad l = 0, 3, \dots, D, \\ \langle \tilde{T}_l^l \rangle_{\text{R}} &= \langle T_l^l \rangle + \frac{(-1)^l (\langle T_1^1 \rangle - \langle T_2^2 \rangle) \sin^2 \theta_1}{(\cosh \chi - \sinh \chi \cos \theta_1)^2}, \quad l = 1, 2. \end{aligned} \quad (5.13)$$

In addition to the diagonal components, the vacuum energy-momentum tensor in the new coordinate system also has a non-zero off-diagonal component

$$\langle \tilde{T}_2^1 \rangle_{\text{R}} = \frac{1 - \coth \chi \cos \theta}{(\coth \chi - \cos \theta)^2} \sin \theta (\langle T_1^1 \rangle - \langle T_2^2 \rangle). \quad (5.14)$$

As expected, the trace of the energy-momentum tensor is not changed under the coordinate transformation.

In the problem without boundaries the vacuum stresses are isotropic,  $\langle T_1^1 \rangle_0 = \langle T_2^2 \rangle_0$ , and we obtain  $\langle \tilde{T}_{\mu}^{\nu} \rangle_{0\text{R}} = \langle T_{\mu}^{\nu} \rangle_0$ . By using the result for  $\langle T_{\mu}^{\nu} \rangle_0$  from [32] and the conformal relation (5.8), for the boundary-free part one gets

$$\langle \tilde{T}_{\mu}^{\nu} \rangle_0 = \langle \tilde{T}_{\mu}^{\nu} \rangle_{\text{G}} + \frac{N[a(\tau)]^{-D-1}}{2^D \pi^{\frac{D}{2}} \Gamma(\frac{D}{2})} \int_0^{\infty} d\omega \frac{\omega^D B_D(\omega)}{e^{2\pi\omega} - (-1)^D} \text{diag} \left( -1, \frac{1}{D}, \dots, \frac{1}{D} \right), \quad (5.15)$$

where  $B_1 = B_2 = 1$  and

$$B_D(\omega) = \prod_{l=1}^{\lfloor \frac{D-1}{2} \rfloor} \left[ 1 + \left( \frac{l - \{\frac{D}{2}\}}{\omega} \right)^2 \right], \quad (5.16)$$

for  $D \geq 3$ . In (5.16),  $\lfloor \frac{D-1}{2} \rfloor$  and  $\{\frac{D}{2}\}$  correspond to the integer and fractional parts of the enclosed numbers, respectively. The spatial geometry under consideration is maximally symmetric and as expected the VEV (5.15) is homogeneous. For the boundary-induced part, from (5.9) we have  $\langle \tilde{T}_{\mu}^{\nu} \rangle_{\text{b}} = [\rho/a(\tau)]^{D+1} \langle \tilde{T}_{\mu}^{\nu} \rangle_{\text{bR}}$ , where the boundary-induced contribution  $\langle \tilde{T}_{\mu}^{\nu} \rangle_{\text{bR}}$  is given by the right-hand sides of (5.13) and (5.14) with replacement  $\langle T_{\mu}^{\nu} \rangle \rightarrow \langle T_{\mu}^{\nu} \rangle_{\text{b}}$ . The boundary-induced vacuum stresses are anisotropic,  $\langle T_1^1 \rangle_{\text{b}} \neq \langle T_2^2 \rangle_{\text{b}}$ , and the off-diagonal component is not zero. By taking into account that for a massless field the combination  $\rho^{D+1} \langle T_{\mu}^{\nu} \rangle_{\text{b}}$  depends on  $\rho$  and  $\rho_0$  through the ratio  $\rho/\rho_0$  (see Eqs. (4.20) and (4.35)), we see that the same holds for the VEV  $\langle \tilde{T}_{\mu}^{\nu} \rangle_{\text{b}}$ . Again, this is a consequence of the homogeneity of the background space. The location of the boundary in the new coordinates is given by

$$\cosh \chi - \sinh \chi \cos \theta_1 = \frac{\rho_0}{\alpha_0}. \quad (5.17)$$

In the theory of the Casimir effect, closed analytical results for vacuum characteristics are usually obtained for boundaries that are coordinate surfaces (e.g., flat, spherical, cylindrical boundaries). As seen from Eq. (5.17), the geometry of the boundary in the example under consideration is quite complicated in terms of the initial coordinates.

Let us consider some special cases of the scale factor in (5.10). For the Milne universe, the scale factor in synchronous time is given by  $a = t$ . In terms of the conformal time  $\tau$ , it is expressed as  $a(\tau) = \alpha e^{\tau}$  with a constant  $\alpha$ . The Milne universe is flat and  $\langle \tilde{T}_{\mu}^{\nu} \rangle_{\text{G}} = 0$ . Another example corresponds to the de Sitter spacetime foliated by hyperbolic coordinates. The corresponding line element is given by (5.10) with  $a^2(\tau) = \alpha^2 / \sinh^2 \tau$ . In terms of the time  $t$ , the scale factor becomes  $a^2 = \alpha^2 \sinh^2(t/\alpha)$ .

## 6 Conclusion

We have studied the fermionic Casimir densities induced by a planar boundary uniformly accelerated through the Fulling-Rindler vacuum state. The boundary separates the right Rindler wedge into two regions: the region between the Rindler horizon and boundary with  $0 < \rho < \rho_0$  (RL region) and the region  $\rho_0 < \rho < \infty$  (RR region). On the boundary the field is constrained by the bag boundary condition and we have found the complete set of corresponding fermionic modes in both regions. The modes are specified by the set of quantum numbers  $(\omega, \mathbf{k}, \eta)$  where  $\mathbf{k}$  is the momentum along the directions perpendicular to the direction of acceleration and  $\eta$  enumerates the spinorial degrees of freedom. The eigenvalues of the energy  $\omega$  are continuous in the RL region. In the RR region, the energy spectrum is discrete and the corresponding eigenvalues are roots of the equation (2.20). For the evaluation of the VEVs of physical observables, bilinear in the field operator, the summation technique over the complete set of modes is employed. The mode sums in the RR region contain a summation over the eigenvalues  $\omega_n = \omega_n(\lambda)$  given implicitly. For the summation of the corresponding series we use a variant of the generalized Abel-Plana formula. This allows to separate the boundary-induced contributions in the VEVs. They are presented in the form of integrals exponentially convergent for points away from the boundary. Similar representations are obtained for the VEVs in the RL region.

As important local characteristics of the fermionic vacuum, we have considered the fermion condensate and the expectation value of the energy-momentum tensor. They are splitted into boundary-free and boundary-induced contributions. For points outside the boundary the renormalization is required for the first parts only. The corresponding renormalized VEVs for a massive field in general number of spatial dimensions were investigated in [32]. The fermion condensate and the vacuum energy-momentum tensor are expressed as (3.8) and (4.16). The vacuum stresses for the Fulling-Rindler vacuum in the boundary-free problem are isotropic. That is not the case for the boundary-induced contributions. For the fermion condensate, those contributions are given by the expressions (3.11) and (3.30) in the RR and RL regions, respectively. The corresponding formulas for the VEV of the energy-momentum tensor are given by (4.13) and (4.32) with the functions  $F_\mu[G_\nu(x)]$  defined in (4.5). We have explicitly checked that the boundary-induced parts in the VEVs obey the covariant conservation equation and the trace relation (4.18). The parallel stresses in the problem on background of  $(D+1)$ -dimensional spacetime are connected with the fermion condensate in  $(D+3)$  dimensional spacetime by simple relations (4.19).

For  $D \geq 2$  the fermion condensate vanishes for a massless field. In the case  $D = 1$ , the condensate for a massless field in the RR region is given by (3.14) and the corresponding expression for the RL region differs by the sign. For a massive field, the boundary-free contribution to the fermion condensate is negative. The boundary-induced part in the fermion condensate is negative in the RR region and positive in the RL region. In the RR region both the boundary-free and boundary-induced parts in the energy density and in the effective pressures along the directions parallel to the mirror,  $-\langle T_l^l \rangle$ ,  $l = 2, 3, \dots, D$ , are negative. In the RL region these VEVs have opposite signs compared to the RR region. Near the mirror, the total VEVs are dominated by the boundary-induced contributions, whereas the boundary-free contributions are dominant near the Rindler horizon. For a massive field, in the RR region and at large distances from the mirror,  $m\rho \gg 1$ , the boundary-induced contribution dominates in the range  $m\rho_0 > 0.04$ .

For a mirror at rest relative to an inertial observer in the Minkowski vacuum the fermion condensate is given by (4.37) and it is negative. The normal stress vanishes and the parallel stresses are equal to the energy density, determined from  $\langle T_0^0 \rangle_{\text{ren}}^{(M)} = m \langle \bar{\psi}\psi \rangle_{\text{ren}}^{(M)} / D$ . For a massless field the VEV of the energy-momentum tensor vanishes and for the fermion condensate one has the expression (4.38). It would also be interesting to compare the above results with the expectation values induced by a mirror moving with constant proper acceleration in the Minkowski vacuum. However, no such investigation has been conducted in the literature. When a mirror moves nonuniformly through the Minkowski vacuum, real particles may be created. This phenomenon is known as the dynamical Casimir effect (see, e.g., [13, 14, 65]). The problem with general law of motion is exactly solvable for conformally invariant fields

in spatial dimension  $D = 1$ . In higher dimensions, different approximate methods have been used. In particular, most investigations consider the nonrelativistic motion of mirrors, including oscillatory motion.

In Section 5, we use the results obtained for the Rindler background spacetime to investigate the fermionic Casimir densities in gravitational fields. Cases involving weak gravitational fields and background geometries that are conformally related to Rindler spacetime are discussed. One such application involves the consideration of the VEV of the energy-momentum tensor in an open cosmological model described by the Friedmann-Robertson-Walker metric. The corresponding conformal image of a planar boundary in Rindler spacetime is rather complicated and the boundary-induced energy-momentum tensor has also a nonzero off-diagonal component.

## Acknowledgments

A.A.S. was supported by the grant No. 21AG-1C047 of the Higher Education and Science Committee of the Ministry of Education, Science, Culture and Sport RA. L.Sh.G. and V.Kh.K. were supported by the grant No. 21AG-1C069 of the Higher Education and Science Committee of the Ministry of Education, Science, Culture and Sport RA.

## A Normalization integral

In this section we evaluate the integrals appearing in the normalization conditions of the fermionic mode functions for the RR and RL regions. The integrals have the form

$$J_{\omega\omega'} = \chi_{\eta'}^{(j)\dagger}(\mathbf{k}) \int_{\rho_1}^{\rho_2} d\rho Z_{i\omega'+\frac{1}{2}\gamma^{(0)}\gamma^{(1)}}(\lambda\rho) Z_{i\omega-\frac{1}{2}\gamma^{(0)}\gamma^{(1)}}(\lambda\rho) \chi_{\eta}^{(+)}(\mathbf{k}), \quad (\text{A.1})$$

where the function  $Z_{\nu}(x)$  is given by (2.4). By using the relation (2.11), we obtain the representation

$$J_{\omega\omega'} = \frac{1}{2} \sum_{\varkappa=\pm 1} \chi_{\eta'}^{(j)\dagger}(\mathbf{k}) \left(1 + \varkappa\gamma^{(0)}\gamma^{(1)}\right) \chi_{\eta}^{(+)}(\mathbf{k}) \int_{\rho_1}^{\rho_2} d\rho Z_{i\omega'+\frac{\varkappa}{2}}(\lambda\rho) Z_{i\omega-\frac{\varkappa}{2}}(\lambda\rho). \quad (\text{A.2})$$

The expression in the right-hand side is further simplified on the base of (2.8) and (2.14):

$$J_{\omega\omega'} = \frac{\delta_{\eta\eta'}}{2\lambda} \int_{\lambda\rho_1}^{\lambda\rho_2} dx \left[ Z_{i\omega'+\frac{1}{2}}(x) Z_{i\omega-\frac{1}{2}}(x) + Z_{i\omega'-\frac{1}{2}}(x) Z_{i\omega+\frac{1}{2}}(x) \right]. \quad (\text{A.3})$$

For the evaluation of the integral in (A.3) we note that the function  $Z_{\nu}(x)$  obeys the equation for the modified Bessel functions. From that equation it follows that (see also [66] for the special case  $Z_{\nu}(x) = K_{\nu}(x)$  and  $x_2 = \infty$ )

$$\int_{x_1}^{x_2} \frac{dx}{x} Z_{\mu}(x) Z_{\nu}(x) = x \frac{Z'_{\mu}(x) Z_{\nu}(x) - Z_{\mu}(x) Z'_{\nu}(x)}{\mu^2 - \nu^2} \Big|_{x=x_1}^{x=x_2}. \quad (\text{A.4})$$

We will assume that the coefficients in (2.4) are taken in the way to have the relation

$$Z_{\mu+1}(x) + Z'_{\mu}(x) = \frac{\mu}{x} Z_{\mu}(x). \quad (\text{A.5})$$

In particular, this relation is obeyed for the functions  $K_{\mu}(x)$  and  $e^{-\mu\pi i} I_{\mu}(x)$ . By using (A.5) in (A.4) we obtain

$$\int_{x_1}^{x_2} dx Z_{\nu}(x) Z_{\mu+1}(x) = \mu x \frac{Z'_{\mu}(x) Z_{\nu}(x) - Z_{\mu}(x) Z'_{\nu}(x)}{\mu^2 - \nu^2} \Big|_{x=x_1}^{x=x_2} - \int_{x_1}^{x_2} dx Z_{\nu}(x) Z'_{\mu}(x). \quad (\text{A.6})$$

From here it follows that

$$\int_{x_1}^{x_2} dx [Z_\mu(x)Z_{\nu+1}(x) + Z_\nu(x)Z_{\mu+1}(x)] = x \frac{Z_\mu(x)Z_{\nu+1}(x) - Z_{\mu+1}(x)Z_\nu(x)}{\mu - \nu} \Big|_{x=x_1}^{x=x_2}. \quad (\text{A.7})$$

Now, in the general formula (A.7) we take  $\mu = i\omega - 1/2$  and  $\nu = i\omega' - 1/2$ :

$$\int_{x_1}^{x_2} dx \sum_{\varkappa=\pm 1} Z_{i\omega-\varkappa/2}(x)Z_{i\omega'+\varkappa/2}(x) = \frac{x}{i} \sum_{\varkappa=\pm 1} \varkappa \frac{Z_{i\omega-\varkappa/2}(x)Z_{i\omega'+\varkappa/2}(x)}{\omega - \omega'} \Big|_{x=x_1}^{x=x_2}. \quad (\text{A.8})$$

With this result, for the integral appearing in the normalization conditions one obtains

$$J_{\omega\omega'} = \delta_{\eta\eta'} \frac{\rho}{2i} \sum_{\varkappa=\pm 1} \varkappa \frac{Z_{i\omega-\varkappa/2}(\lambda\rho)Z_{i\omega'+\varkappa/2}(\lambda\rho)}{\omega - \omega'} \Big|_{\rho=\rho_1}^{\rho=\rho_2}. \quad (\text{A.9})$$

This result is used in the main text for the evaluation of the normalization coefficients in the RR and RL regions.

## B Summation formula over the eigenmodes in the RR region

In this section we derive a summation formula over the eigenmodes  $z = \omega_n$  being the roots of the function  $\bar{K}_{iz+1/2}(u)$ . For that the generalized Abel-Plana formula from [67] will be used. In the generalized Abel-Plana formula we take

$$\begin{aligned} f(z) &= \frac{2}{\pi} \cosh \pi z F(z), \\ g(z) &= \frac{\bar{I}_{iz+1/2}(\eta) - \bar{I}_{-iz+1/2}(\eta)}{\bar{K}_{iz+1/2}(\eta)} F(z), \end{aligned} \quad (\text{B.1})$$

where  $F(z)$  is a function analytic in the right-half plane  $\text{Re } z > 0$  and the functions with bar are defined in (2.26) and (2.28). For the sum and difference of these functions one has

$$g(z) \pm f(z) = \mp 2 \frac{\bar{I}_{\mp iz+1/2}(\eta)}{\bar{K}_{iz+1/2}(\eta)} F(z). \quad (\text{B.2})$$

By taking into account that

$$\bar{I}_{-i\omega_n+1/2}(u) = -\bar{I}_{i\omega_n+1/2}(u), \quad (\text{B.3})$$

for the residues of the function  $g(z)$  at the points  $z = \omega_n$  we obtain

$$\text{Res}_{z=\omega_n} g(z) = \frac{2\bar{I}_{iz+1/2}(u)}{\partial_z \bar{K}_{iz+1/2}(u)} F(z) \Big|_{z=\omega_n}. \quad (\text{B.4})$$

Plugging (B.2) and (B.4) in the generalized Abel-Plana formula [67], the formula

$$\begin{aligned} \lim_{h \rightarrow \infty} \left[ \sum_{n=1}^{n_h} \frac{i\bar{I}_{iz+1/2}(u)F(z)}{\partial_z \bar{K}_{iz+1/2}(u)} \Big|_{z=\omega_n} - \frac{1}{\pi^2} \int_0^h dx \cosh(\pi x) F(x) \right] \\ = \frac{i}{2\pi} \int_0^\infty dx \frac{\bar{I}_{x+1/2}(u)}{\bar{K}_{x+1/2}(u)} \left[ F(xe^{\frac{\pi i}{2}}) - F(xe^{-\frac{\pi i}{2}}) \right], \end{aligned} \quad (\text{B.5})$$

is obtained. Here, for a given  $h$ , the upper limit of the summation is defined in accordance with  $\omega_{n_h} < h < \omega_{n_h+1}$ . From the conditions on the functions  $f(z)$  and  $g(z)$  in the generalized Abel-Plana formula we get the condition on the function  $F(z)$  in (B.5). For  $z = x + iy$ , with  $x > 0$ , it takes the form

$$|F(z)| < \varepsilon(|z|)e^{-\pi x}(|z|/u)^{2|y|}, \quad (\text{B.6})$$

for large values of  $|z|$ , where  $|z|\varepsilon(|z|) \rightarrow 0$  in the limit  $|z| \rightarrow 0$ . From (B.3) it follows that the function  $i\bar{I}_{i\omega_n+1/2}(\eta)$  is real. Note that we have the relation

$$\bar{I}_{i\omega_n+1/2}(u) = -\frac{1}{uK_{i\omega_n+1/2}(u)}, \quad (\text{B.7})$$

and the function  $iK_{i\omega_n+1/2}(u)$  is also real. Modes of quantum fields expressed in terms of the modified Bessel function of the second kind with an imaginary order appear also in other background geometries. An example of a (2+1)-dimensional spacetime is the Beltrami pseudosphere (see [68] for the corresponding vacuum currents). The summation formula (B.5) can be used to investigate edge-induced effects in these geometries.

## C Proof of the identities

In this section, the proof of the identity (3.26) is presented. By taking into account the relation (3.25), we can write

$$\frac{Z_{\nu_{\pm}}^2(u)}{|C_{\sigma}|^2} = \frac{Z_{\nu_{\pm}}(u)}{C_{\sigma}} \left[ \frac{Z_{\nu_{\mp}}(u)}{C_{\sigma}} \right]^*, \quad (\text{C.1})$$

with  $u = \lambda\rho$  and

$$\nu_{\pm} = i\omega \pm \frac{1}{2}. \quad (\text{C.2})$$

Substituting the expression (3.24) for the functions  $Z_{i\omega_{\pm}\frac{1}{2}}(u)$  it can be seen that

$$\begin{aligned} \frac{Z_{\nu_{\pm}}^2(u)}{|C_{\sigma}|^2} &= K_{\nu_{\pm}}^2(u) - \bar{K}_{\nu_{+}}(u_0) \left\{ \frac{I_{\nu_{\pm}}(u)}{\bar{I}_{\nu_{+}}(u_0)} \frac{I_{-\nu_{\pm}}(u)}{\bar{I}_{-\nu_{-}}(u_0)} \bar{K}_{\nu_{+}}(u_0) \right. \\ &\quad \left. \pm \left[ \frac{I_{\nu_{\pm}}(u)}{\bar{I}_{\nu_{+}}(u_0)} - \frac{I_{-\nu_{\pm}}(u)}{\bar{I}_{-\nu_{-}}(u_0)} \right] K_{\nu_{+}}(u) \right\}, \end{aligned} \quad (\text{C.3})$$

where  $u_0 = \lambda\rho_0$ . Next, we use the relations

$$\begin{aligned} \bar{K}_{\nu_{+}}(z) &= -\pi \frac{\bar{I}_{-\nu_{-}}(z) + \bar{I}_{\nu_{+}}(z)}{2 \cosh(\omega\pi)}, \\ K_{\nu_{\pm}}(u) &= \pm\pi \frac{I_{-\nu_{\pm}}(u) - I_{\nu_{\pm}}(u)}{2 \cosh(\omega\pi)}, \end{aligned} \quad (\text{C.4})$$

to show that

$$\frac{Z_{\nu_{\pm}}^2(\lambda\rho)}{|C_{\sigma}|^2} - K_{\nu_{\pm}}^2(\lambda\rho) = \frac{\pi \bar{K}_{\nu_{+}}(z)}{2 \cosh(\omega\pi)} \left[ \frac{I_{\nu_{\pm}}^2(\lambda\rho)}{\bar{I}_{\nu_{+}}(z)} + \frac{I_{-\nu_{\pm}}^2(\lambda\rho)}{\bar{I}_{-\nu_{-}}(z)} \right]. \quad (\text{C.5})$$

The identity (3.26) is a direct consequence of this relation.

In order to evaluate the boundary-induced contribution in the VEV of the energy density in the RL region, we need to have the analog of the identity (C.5) for the product  $Z_{i\omega+1/2}(u) Z_{i\omega-1/2}(u)$ . In the way similar to that used for (C.5), by using the relations (C.4), it can be shown that

$$\frac{Z_{\nu_{+}}(u) Z_{\nu_{-}}(u)}{|C_{\sigma}|^2} = K_{\nu_{+}}(u) K_{\nu_{-}}(u) - \frac{\pi \bar{K}_{\nu_{+}}(u_0)}{2 \cosh(\omega\pi)} \sum_{j=\pm 1} \frac{I_{ji\omega-\frac{1}{2}}(u) I_{ji\omega+\frac{1}{2}}(u)}{\bar{I}_{ji\omega+1/2}(u_0)}. \quad (\text{C.6})$$

In order to obtain a similar identity for the function entering in the expression of the stress  $\langle T_1^1 \rangle$ , we use the relation

$$Z_{\nu_-}(z) Z'_{\nu_+}(z) - Z_{\nu_+}(z) Z'_{\nu_-}(z) = Z_{\nu_+}^2(z) - Z_{\nu_-}^2(z) - 2\frac{i\omega}{z} Z_{\nu_+}(z) K_{\nu_-}(z), \quad (\text{C.7})$$

and the identities for the separate parts in the right-hand side, given above.

## References

- [1] N. D. Birrell and P. C. W. Davies, *Quantum Fields in Curved Space* (Cambridge University Press, Cambridge, England, 1982).
- [2] L. C. B. Crispino, A. Higuchi, and G. E. A. Matsas, The Unruh effect and its applications, *Rev. Mod. Phys.* **80**, 787 (2008).
- [3] P. P. Langlois, Imprints of spacetime topology in the Hawking-Unruh effect, arXiv:gr-qc/0510127.
- [4] S. A. Fulling, Nonuniqueness of canonical field quantization in Riemannian space-time, *Phys. Rev. D* **7**, 2850 (1973).
- [5] P. C. W. Davies, Scalar production in Schwarzschild and Rindler metrics, *J. Phys. A: Math. Gen.* **8**, 609 (1975).
- [6] W. G. Unruh, Notes on black-hole evaporation, *Phys. Rev. D* **14**, 870 (1976).
- [7] I. Fuentes-Schuller and R. B. Mann, Alice falls into a black hole: Entanglement in noninertial frames, *Phys. Rev. Lett.* **95**, 120404 (2005).
- [8] P. M. Alsing, I. Fuentes-Schuller, R. B. Mann, and T. E. Tessier, Entanglement of Dirac fields in noninertial frames, *Phys. Rev. A* **74**, 032326 (2006).
- [9] K. Ueda, A. Higuchi, K. Yamamoto, A. Rohim, and Y. Nan, Entanglement of the vacuum between left, right, future, and past: Dirac spinor in Rindler and Kasner spaces, *Phys. Rev. D* **103**, 125005 (2021).
- [10] J. Yan and B. Zhang, Effect of spacetime dimensions on quantum entanglement between two uniformly accelerated atoms, *J. High Energy Phys.* 10 (2022) 051.
- [11] V. M. Mostepanenko and N. N. Trunov, *The Casimir Effect and Its Applications* (Clarendon, Oxford, 1997).
- [12] K. A. Milton, *The Casimir Effect: Physical Manifestation of Zero-Point Energy* (World Scientific, Singapore, 2002).
- [13] M. Bordag, G. L. Klimchitskaya, U. Mohideen, and V. M. Mostepanenko, *Advances in the Casimir Effect* (Oxford University Press, New York, 2009).
- [14] *Casimir Physics*, edited by D. Dalvit, P. Milonni, D. Roberts, and F. da Rosa, Lecture Notes in Physics Vol. 834 (Springer-Verlag, Berlin, 2011).
- [15] P. Candelas and D. Deutsch, Fermion fields in accelerated states, *Proc. R. Soc. Lond. A* **362**, 251 (1978).
- [16] M. Soffel, B. Müller, and W. Greiner, Dirac particles in Rindler space, *Phys. Rev. D* **22**, 1935 (1980).

- [17] S. Tagaki, On the response of a Rindler particle detector. III, *Prog. Theor. Phys.* **74**, 501 (1985).
- [18] S. Tagaki, Vacuum noise and stress induced by uniform acceleration, *Prog. Theor. Phys. Suppl.* **88**, 1 (1986).
- [19] R. Járegui, M. Torres, and S. Hacyan, Dirac vacuum: Acceleration and external-field effects, *Phys. Rev. D* **43**, 3979 (1991).
- [20] E. Bautista, Acceleration through the Dirac-Pauli vacuum and effects of an external field, *Phys. Rev. D* **48**, 783 (1993).
- [21] V. Moretti and L. Vanzo, Thermal Wightman functions and renormalized stress tensors in the Rindler wedge, *Phys. Lett. B* **375**, 54 (1996).
- [22] D. Oriti, The spinor field in Rindler spacetime: An analysis of the Unruh effect, *Nuovo Cimento della Societa Italiana di Fisica B* **115**, 1005 (2000).
- [23] D. A. T. Vanzella and G. E. A. Matsas, Decay of accelerated protons and the existence of the Fulling-Davies-Unruh Effect, *Phys. Rev. Lett.* **87**, 151301 (2001).
- [24] P. P. Langlois, Causal particle detectors and topology, *Ann. Phys.* **321**, 2027 (2006).
- [25] C. H. G. Bessa, J. G. Dueñas, and N. F. Svaiter, Accelerated detectors in Dirac vacuum: the effects of horizon fluctuations. *Class. Quantum Grav.* **29**, 215011 (2012).
- [26] W. Zhou and H. Yu, Spontaneous excitation of a uniformly accelerated atom coupled to vacuum Dirac field fluctuations, *Phys. Rev. A* **86**, 033841 (2012).
- [27] J. Louko and V. Toussaint, Unruh-DeWitt detector's response to fermions in flat spacetimes, *Phys. Rev. D* **94**, 064027 (2016).
- [28] D. Hümmer, E. Martín-Martínez, and A. Kempf, Renormalized Unruh-DeWitt particle detector models for boson and fermion fields, *Phys. Rev. D* **93**, 024019 (2016).
- [29] S. Kaushal, Schwinger effect and a uniformly accelerated observer, *Eur. Phys. J. C* **82**, 872 (2022).
- [30] V. Kh. Kotanjyan, A. A. Saharian, and M. R. Setare, Vacuum currents in partially compactified Rindler spacetime with an application to cylindrical black holes, *Nucl. Phys. B* **980**, 115838 (2022).
- [31] R. Falcone and C. Conti, Minkowski vacuum in Rindler spacetime and Unruh thermal state for Dirac fields, *Phys. Rev. D* **107**, 105021 (2023).
- [32] S. Bellucci, V. Kh. Kotanjyan, and A. A. Saharian, Fermionic condensate and the mean energy-momentum tensor in the Fulling-Rindler vacuum. *Phys. Rev. D* **108**, 085014 (2023).
- [33] P. Candelas and D. Deutsch, On the vacuum stress induced by uniform acceleration or supporting the ether, *Proc. R. Soc. Lond. A* **354**, 79 (1977).
- [34] A. A. Saharian, Polarization of the Fulling-Rindler vacuum by a uniformly accelerated mirror, *Class. Quantum Grav.* **19**, 5039 (2002).
- [35] R. M. Avagyan, A. A. Saharian, and A. H. Yeranyan, Casimir effect in the Fulling-Rindler vacuum, *Phys. Rev. D* **66**, 085023 (2002).
- [36] A. A. Saharian, R. S. Davtyan, and A. H. Yeranyan, Casimir energy in the Fulling-Rindler vacuum, *Phys. Rev. D* **69**, 085002 (2004).

- [37] A. A. Saharian and M. R. Setare, Surface vacuum energy and stresses on a plate uniformly accelerated through the Fulling-Rindler vacuum, *Class. Quantum Gravity* **21**, 5261 (2004).
- [38] A. A. Saharian, R. M. Avagyan, and R. S. Davtyan, Wightman function and Casimir densities for Robin plates in the Fulling-Rindler vacuum, *Int. J. Mod. Phys. A* **21**, 2353 (2006).
- [39] G. Bimonte, E. Calloni, G. Esposito, and L. Rosa, Energy-momentum tensor for a Casimir apparatus in a weak gravitational field. *Phys. Rev. D* **74**, 085011 (2006); **77**, 109903(E) (2008).
- [40] S. A. Fulling, K. A. Milton, P. Parashar, A. Romeo, K. V. Shajesh, and J. Wagner, How does Casimir energy fall? *Phys. Rev. D* **76**, 025004 (2007).
- [41] K. A. Milton, P. Parashar, K. V. Shajesh, and J. Wagner, How does Casimir energy fall? II. Gravitational acceleration of quantum vacuum energy. *J. Phys. A* **40**, 10935 (2007).
- [42] K. V. Shajesh, K. A. Milton, P. Parashar, and J. A. Wagner, How does Casimir energy fall? III. Inertial forces on vacuum energy. *J. Phys. A* **41**, 164058 (2008).
- [43] K. A. Milton, K. V. Shajesh, S. A. Fulling, P. Parashar, How does Casimir energy fall? IV. Gravitational interaction of regularized quantum vacuum energy. *Phys. Rev. D* **89**, 064027 (2014).
- [44] G. Lambiase, A. Stabile, and An. Stabile, Casimir effect in extended theories of gravity. *Phys. Rev. D* **95**, 084019 (2017).
- [45] F. Sorge and J. H. Wilson, Casimir effect in free-fall towards a Schwarzschild black hole, *Phys. Rev. D* **100**, 105007 (2019).
- [46] L. Buoninfante, G. Lambiase, L. Petruzzello, A. Stabile, Casimir effect in quadratic theories of gravity. *Eur. Phys. J. C* **79**, 41 (2019).
- [47] A. P. C. M Lima, G. Alencar, C. R. Muniz, and R. R. Landim, Null second order corrections to Casimir energy in weak gravitational field. *JCAP07(2019)011*.
- [48] J. H. Wilson, F. Sorge, and S. A. Fulling, Tidal and nonequilibrium Casimir effects in free fall. *Phys. Rev. D* **101**, 065007 (2020).
- [49] F. Sorge, Quasi-local Casimir energy and vacuum buoyancy in a weak gravitational field. *Class. Quantum Grav.* **38**, 025009 (2021).
- [50] V. B. Bezerra, H. F. S. Mota, A. P. C. M. Lima, G. Alencar, and C. R. Muniz, The Casimir effect in finite-temperature and gravitational scenarios, *Physics* **6**, 1046 (2024).
- [51] K. Shimizu, C, P and T transformations in higher dimensions, *Prog. Theor. Phys.* **74**, 610 (1985).
- [52] L. Parker and J. D. Toms, *Quantum Field Theory in Curved Spacetime: Quantized Fields and Gravity* (Cambridge University Press, Cambridge, England, 2009).
- [53] *Handbook of Mathematical Functions*, edited by M. Abramowitz and I. A. Stegun (Dover, New York, 1972).
- [54] E. Elizalde, S. D. Odintsov, and A. A. Saharian, Fermionic condensate and Casimir densities in the presence of compact dimensions with applications to nanotubes. *Phys. Rev. D* **83**, 105023 (2011).
- [55] S. Bellucci and A. A. Saharian, Fermionic Casimir effect for parallel plates in the presence of compact dimensions with applications to nanotubes, *Phys. Rev. D* **80**, 105003 (2009).

- [56] S. Bellucci and A. A. Saharian, Fermionic current from topology and boundaries with applications to higher-dimensional models and nanophysics, *Phys. Rev. D* **87**, 025005 (2013).
- [57] S. Bellucci, W. Oliveira dos Santos, E. R. Bezerra de Mello, and A. A. Saharian, Cosmic string and brane induced effects on the fermionic vacuum in AdS spacetime, *J. High Energy Phys.* 05 (2022) 021.
- [58] V. P. Gusynin, S. G. Sharapov, and J. P. Carbotte, AC conductivity of graphene: From tight-binding model to 2 + 1-dimensional quantum electrodynamics, *Int. J. Mod. Phys. B* **21**, 4611 (2007).
- [59] A. H. Castro Neto, F. Guinea, N. M. R. Peres, K. S. Novoselov, and A. K. Geim, The electronic properties of graphene, *Rev. Mod. Phys.* **81**, 109 (2009).
- [60] O. Vafek and A. Vishwanath, Dirac fermions in solids: From High-Tc cuprates and graphene to topological insulators and Weyl semimetals, *Annu. Rev. Condens. Matter Phys.* **5**, 83 (2014).
- [61] A. Iorio and G. Lambiase, The Hawking-Unruh phenomenon on graphene, *Phys. Lett. B* **716**, 334 (2012).
- [62] A. Iorio and G. Lambiase, Quantum field theory in curved graphene spacetimes, Lobachevsky geometry, Weyl symmetry, Hawking effect, and all that, *Phys. Rev. D* **90**, 025006 (2014).
- [63] A. Bhardwaj and D. E. Sheehy, Unruh effect and Takagi's statistics inversion in strained graphene, *Phys. Rev. D* **107**, 224310 (2023).
- [64] R. Emparan and H. S. Reall, black holes in higher dimensions, *Living Rev. Rel.* **11**, 6 (2008).
- [65] V. V. Dodonov, Dynamical Casimir effect: 55 years later, *Physics* **7**, 10 (2025).
- [66] A. P. Prudnikov, Yu. A. Brychkov, and O. I. Marichev, *Integrals and Series* (Gordon and Breach, New York, 1986), Vol. 2.
- [67] A. A. Saharian, *The Generalized Abel-Plana Formula with Applications to Bessel Functions and Casimir Effect* (Yerevan State University Publishing House, Yerevan, 2008) (arXiv:0708.1187).
- [68] A. A. Saharian, Vacuum currents in curved tubes, *Phys. Rev. D* **110**, 065020 (2024).